



PII S0016-7037(01)00724-4

Dissolution of nepheline, jadeite and albite glasses: Toward better models for aluminosilicate dissolution

JAMES P. HAMILTON,^{1,†} SUSAN L. BRANTLEY,^{2,*} CARLO G. PANTANO,¹ LOUISE J. CRISCENTI,² and JAMES D. KUBICKI²

¹Department of Materials Science and Engineering, Pennsylvania State University, University Park, PA 16802, USA

²Department of Geosciences, Pennsylvania State University, University Park, PA 16802, USA

(Received February 12, 2001; accepted in revised form June 20, 2001)

Abstract—SLB acknowledges many educational and entertaining conversations with Hal Helgeson (ranging from kinetics to bent head morphologies) over the last 17 years.

To investigate the effects of changing the Al/Si ratio on plagioclase dissolution without complications of varying Na/Ca content or exsolution, three glasses with varying Al/Si ratios (albite, jadeite, and nepheline glasses) were synthesized and dissolved. Many similarities in dissolution behavior between plagioclase crystals and this suite of glasses were observed: 1) dissolution was slowest at near-neutral pH and increased under acid and basic conditions; 2) dissolution rate at all pH values increased with increasing Al/Si ratio; 3) the pH dependence of dissolution was higher for the phase with Al/Si = 1 than the phase with Al/Si = 0.3; 4) after acid leaching, the extent of Al depletion of the altered surface increased with increasing bulk Al/Si ratio from Al/Si = 0.3 (albite glass) to 0.5 (jadeite glass), but then decreased in nepheline glass (Al/Si = 1.0), which dissolved stoichiometrically with respect to Al; and 5) little to no Al depletion of the surface of any glass occurred at pH > 7. In contrast with some observations for plagioclase dissolution, however, log (rate) increased linearly with Al content, and *n*, the slope of the log (rate) – pH curve at low pH, varied smoothly from albite glass to jadeite glass to nepheline glass (*n* = –0.3, –0.6, and –1.0, respectively). These results, plus the observation that the slope calculated at high pH, *m*, did not differ between glasses (*m* = 0.4 ± 0.1), may be consistent with an identical mechanism controlling dissolution of albite, jadeite, and nepheline glasses, although no Si-rich layer can develop on nepheline because of the lack of SiOSi linkages. Such a conclusion is consistent with a transition state for these aluminosilicates at high pH consisting of a deprotonated Q₃^{Si} hydroxyl group (where Q_v^x refers to an *x* atom in a tetrahedral site with *v* bridging oxygens) or a five-coordinate Si site after nucleophilic attack by OH[–]. At low pH, bridging oxygens between Q₄^{Si} and Q₄^{Al} may be rate limiting if they are slower to hydrolyze than Q_v^{Si}Q_w^{Si} linkages (*v*, *w* ≤ 3). According to this mechanism, dissolution rate increases from albite to jadeite to nepheline glass because hydrolysis of AlOSi bonds become more energetically favorable as the number of Al atoms per Si tetrahedron increases, a phenomenon documented here by geometry optimizations by use of ab initio methods. A model wherein Q₄^{Al}Q₄^{Si} linkages are faster to hydrolyze than lower connectivity linkages between Si atoms (Q_v^{Si}Q_w^{Si}, *v*, *w* ≤ 3) may also explain aspects of this data. Further computational and experimental measurements are needed to distinguish the models. Copyright © 2001 Elsevier Science Ltd

1. INTRODUCTION

The rates of weathering of the most common mineral in the earth's crust, plagioclase, is of interest in fields ranging from agronomy to earthquake engineering, and many discussions of the mechanism of feldspar weathering have been published over these last seventy years (see Helgeson (1971) for early references). The dissolution rate of plagioclase feldspar in the laboratory is relatively fast under acid and basic conditions and slow at near-neutral pH conditions (e.g., Blum and Stillings, 1995; Schott and Oelkers, 1995). As reviewed by Blum and Stillings (1995), under acid conditions (pH 2 and 3) at ambient temperature, the log (dissolution rate) for plagioclase feldspar increases linearly with increasing anorthite content from An0 to An80; however, the rate of dissolution of An100 is significantly faster and lies off these trends (e.g., Fleer, 1982; Chou and Wollast, 1985; Holdren and Speyer, 1987; Mast and Drever, 1987; Amrhein and Suarez, 1988, 1992; Sjöberg, 1989; Sver-

drup, 1990; Casey et al., 1991; Oxburgh et al., 1994; Stillings and Brantley, 1995). At pH 5, a similar trend may be observed, although the reproducibility of rates in the literature is poor. According to Blum and Stillings (and data from papers cited above), when dissolution data measured at pH < neutral are fit to the equation

$$\text{Log rate} = \log k + n \text{ pH} \quad (1)$$

where the value of *n* = –0.5 from An0 to An70, but increases to about –0.75 at An76 and –1.0 at An100, the results suggest that a threshold Al content exists such that dissolution behavior changes drastically.

The increase in dissolution rate observed above an Al threshold concentration of An70 to 80 for plagioclase compositions has been attributed by Blum and Stillings (1995) to the fact that at high Al content, hydrolysis of SiOSi linkages is no longer rate controlling. Oelkers and Schott (1995) further developed a model suggesting that different mechanisms control dissolution for feldspars with <70% and >70% An content. For low An compositions, they argue that formation of a SiOSi-linked, silica-rich precursor complex controls dissolution, but that for

* Author to whom correspondence should be addressed (brantley@geosc.psu.edu).

† Present address: Johns Manville Inc., Littleton, CO 80162, USA.

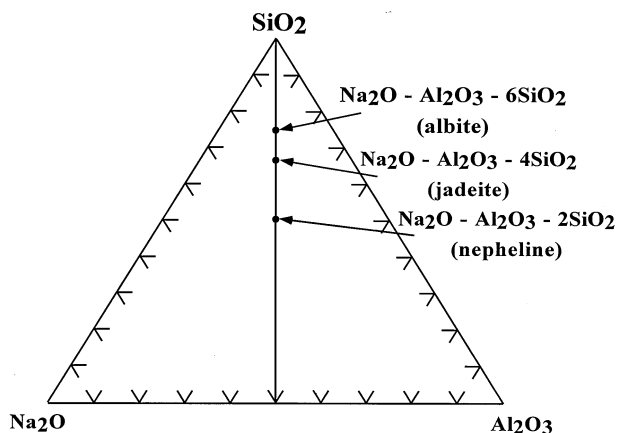


Fig. 1. $\text{Na}_2\text{O}-\text{Al}_2\text{O}_3-\text{SiO}_2$ ternary phase diagram illustrating the $\text{Na}_2\text{O}-\text{Al}_2\text{O}_3-y\text{SiO}_2$ glass system.

compositions more An rich than An70, no such *SiOSi*-linked precursor controls dissolution. For these An-rich compositions, Al ions are preferentially attacked and removed, leaving isolated silica tetrahedra.

One problem with investigating the rate of dissolution of plagioclase feldspars is the presence of exsolution and crystal-line defects in all known plagioclase crystals. Given the similarity between rates of glass and crystal dissolution described by Hamilton et al. (2000) for albite at low, neutral, and high pH, a better matrix for investigation might consist of glass with variable Al/Si content. Indeed, Dubrovo (1954a) observed an increase in dissolution rate for glasses along the disilicate-nepheline join ($\text{Na}_2\text{O}-x\text{Al}_2\text{O}_3-2\text{SiO}_2$) with large increases in alumina content ($x \geq 0.4$) and attributed the effect to an increase in the number of *AlOSi* bonds in the glass network. He proposed that as Al leached out of an aluminosilicate glass with high alumina content, the remaining SiO_4 tetrahedra became isolated (or existed in small aggregates) and were easily decomposed. These observations are similar to observations for dissolution of crystals along the plagioclase join, suggesting that dissolution of aluminosilicate glass might be useful in elucidating the mechanism of dissolution of feldspars. However, in plagioclase glass (as in the crystalline solid solution), Al content changes along with Ca content. To investigate the effect of changing the Al/Si ratio on dissolution of silicates without the added complication of variable Na/Ca ratio or the presence of exsolution lamellae and other crystalline defects found in all plagioclase feldspars, three glasses with variable Al/Si, $\text{NaAlSi}_3\text{O}_8$, $\text{NaAlSi}_2\text{O}_6$, and NaAlSiO_4 (Fig. 1, Table 1), were therefore synthesized. These three glasses are also of interest because they have mineral analogs: albite, jadeite, and nepheline, respectively.

Despite identical chemistry, glass and crystal along this compositional join show differences in short- and long-range order. On the basis of published structure models of alkali-aluminosilicate glasses, albite, jadeite, and nepheline glasses are fully polymerized, containing few or no nonbridging oxygens and containing Si and Al only in tetrahedral coordination (Brückner et al., 1978; Shelby, 1978; Smets and Lommen, 1981; Onorato et al., 1985; Goldman, 1986; Hsieh et al., 1994). Experimentally measured X-ray radial distribution functions

(Taylor and Brown, 1979a) indicate albite glass and crystal consist of predominantly six- or four-membered rings of Si and Al tetrahedra, respectively. However, molecular orbital calculations and Raman spectroscopy of albite glass indicate the possible presence of three-, four-, and six-membered rings (Kubicki and Sykes, 1993; Sykes and Kubicki, 1996). Molecular dynamics simulations indicate ring sizes of 2 to >8 in fully polymerized sodium-aluminosilicate glasses such as albite, nepheline, and jadeite (Zirl and Garofalini, 1990). In contrast, nepheline crystal contains Si and Al in tetrahedral coordination configured in six-membered rings, whereas jadeite crystal contains Si tetrahedrally coordinated in single chains, with Al and Na in octahedral coordination.

Despite differences in structure, Al is generally expected to follow the Al avoidance principle for glasses and crystals with tetrahedrally coordinated Al (Loewenstein, 1954). Only very occasional *AlOAl* linkages (Zirl and Garofalini, 1990; Dirken et al., 1997; Lee and Stebbins, 1999) or no such linkages are expected to form in crystals and glasses for relatively low Al/Si ratios such as albite, jadeite, and nepheline. Glasses of these compositions should therefore provide insight into the effect of variable Al/Si ratio on the dissolution behavior of plagioclase crystals.

Although flow experiments are preferable to batch experiments in terms of ease of interpretation of absolute rates of dissolution (White and Brantley, 1995), it was our intent here to investigate trends in dissolution as a function of pH and composition, and we therefore measured rates of dissolution of these glasses in batch mode. Batch experiments allowed investigation of a full range of pH for all three glasses under identical experimental conditions. Inductively coupled plasma-atomic emission spectroscopy (ICP-AES) and -mass spectrometry (ICP-MS) were used to monitor solution chemistry, and X-ray photoelectron spectroscopy (XPS), secondary ion mass spectrometry (SIMS), and Fourier transform infrared reflection spectroscopy (FTIRRS) were used to study the composition and structure of the glass surfaces.

2. EXPERIMENTAL PROCEDURES

2.1. Sample Preparation

Raw materials for glass melting included Min-U-Sil SiO_2 , reagent-grade $\text{Al}(\text{OH})_3$, anhydrous Na_2CO_3 , and Na_2SO_4 powders (J. T. Baker). Batches (150 g) of each composition were melted in platinum/rhodium crucibles at temperatures ranging from 1700 to 1750°C in air (Table 1). The glasses were melted for 24 h and then poured into stainless steel molds to form bars. The glasses were annealed overnight at temperatures ranging from 690 to 750°C (Table 1) and cooled slowly to room temperature. Spectrochemical analyses of these glasses (based on a lithium metaborate fusion followed by ICP-AES analysis of the resulting solution) indicated only minor deviation from their batch compositions (Table 1). Analysis of annealed starting materials by polariscope and X-ray diffraction revealed no evidence for stress or crystallization, respectively.

Glass plates approximately $2 \times 1 \times 0.2$ cm were cut, and one face was polished to $0.1 \mu\text{m}$ (oil-based diamond sprays), with a final $0.05 \mu\text{m}$ cerium oxide/chrome oxide polishing step. After polishing, the samples were ultrasonically cleaned in acetone for 15 min and the surface concentration of adventitious hydrocarbons was reduced by a 30 min ultraviolet ozone cleaning process (Fig. 1992). Finally, the glass plates were etched in a 1 N NaOH solution at 80°C for 3 min to remove the damaged or contaminated surface layer due to polishing. After this etching procedure, the samples were immediately rinsed in reverse-osmosis-filtered (RO) water at 80°C and blown with nitrogen

Table 1. Spectrochemical characterization of glass powders.^a

Composition designation	Na ₂ O (mole %)	Al ₂ O ₃ (mole %)	SiO ₂ (mole %)	Na (atomic %)	Al (atomic %)	Si (atomic %)	O (atomic %)	Na/Si	Al/Si	Na/Al	Melting temp. (°C)	Annealing temp. (°C)	Al-O-Si linkages per SiO ₄ tetrahedron ^b	Si-O-Si linkages per SiO ₄ tetrahedron ^b	Density (g/cm ³)	Formula unit based on 24 oxygens
Nepheline glass	25.0	25.0	50.0	14.3	14.3	14.3	57.1	1.00	1.00	1.00	1700	690	4.00	0.00	2.496 ^c	Na _{6.01} Al _{6.01} Si _{6.01} O _{24.00}
Jadeite glass	16.8	16.9	66.3	10.0	10.1	19.9	60.0	0.50	0.51	0.99	1750	730	2.03	1.97	2.431 ^d	Na _{4.00} Al _{4.04} Si _{7.96} O _{24.00}
Albite glass	12.6	12.7	74.8	7.7	7.8	23.0	61.5	0.33	0.34	0.99	1750	750	1.36	2.64	2.382 ^d	Na _{3.00} Al _{3.04} Si _{8.98} O _{24.00}

^a Based on a lithium metaborate fusion process followed by ICP-AES analysis of the resulting solution.

^b On the basis of atomic percentages of Al and Si as measured by ICP-AES.

^c Day and Rindone (1962).

^d Taylor and Brown (1979b).

gas. Before exposure to aqueous solutions, the samples were treated by ultraviolet ozone cleaning again for 30 min.

Glass samples were also dry-crushed to a 74- to 149- μm grain size (100 to 200 mesh) in an agate mortar and subsequently cleaned in high-purity acetone and dried at 60°C overnight. Surface areas of powders were measured before dissolution with a standard multipoint BET gas adsorption technique by use of Kr (Micromeritics ASAP 2000). Because of the low surface area, surface area measurements were near the lower limit of the technique and were estimated to be accurate within $\pm 35\%$.

2.2. Reactors

The glass powders were placed in 2-L high-density polyethylene (HDPE) containers and immersed in 2300 mL solution (maximum capacity of containers) for varying durations. These containers were pre-cleaned in hydrochloric acid, nitric acid, and boiling RO water. The containers were placed in an oven maintained at $25 \pm 1^\circ\text{C}$ without agitation. The glass surface area to solution volume ratio (SA/V) was approximately 1.4 to 2.0 cm^{-1} for each experiment. Solutions at pH 1, 2, 4, and 6.4 were prepared with RO water with or without ultrapure HCl. Solutions at pH 9 and 12 were prepared from LiOH and RO water. Although pH changed during the experiments, the experiments are noted throughout this article by the initial pH value.

Twenty-five-milliliter aliquots of solution were collected at various times (at least five time points) during the course of each experiment. Fresh solution was added to each container to maintain a constant SA/V ratio throughout the experiment. After reaction, solutions were filtered through 0.4- μm filter paper, and powders were rinsed with deionized water, ultrasonicated in high-purity acetone, and dried at 50°C overnight.

The polished glass plates were placed in polyfluorotetraethylene baskets that hung vertically in 2300 mL solution from the top of another set of 2-L HDPE containers. These containers were also pre-cleaned in hydrochloric acid, nitric acid, and boiling RO water. The reactors were completely filled with solutions at pH 1, 2, 4, 6.4, 9, and 12 and sealed with Parafilm. This procedure prevented the pH from drifting more than 0.3 pH units over 1000 h. The glass specimens were immersed in these solutions for varying durations of 1 to 1100 h. The containers were placed in an oven maintained at $25 \pm 1^\circ\text{C}$ without agitation. The SA/V was approximately $5.0 \times 10^{-3}\text{ cm}^{-1}$ for each batch experiment. After reaction, the samples were rinsed in high-purity acetone, blown with nitrogen gas, and stored in a vacuum desiccator for surface analysis.

2.3. Postreaction Analysis

2.3.1. Solution Analysis

Solutions from the experiments conducted with powdered specimens at pH 1, 2, 4, and 12 were filtered to 0.4 μm and analyzed for Na, Al, and Si with a Leeman Labs PS ICP-AES. Solutions from the experiments conducted at pH 6.4 (water) and 9 were analyzed with a Finnigan MAT, double-focusing sector field ICP-MS. Solution pH was monitored with an Orion Research 611 pH meter with an Orion Ross combination pH electrode with an accuracy of ± 0.01 pH units.

2.3.2. XPS

The outermost 90 Å of the glass surfaces was analyzed via XPS with a Kratos XSAM 800 spectrometer. Nonmonochromatic, MgK_α X-rays were used with an anode current of 20 mA at an electron acceleration voltage of 14 kV. The pass energy was set at 40 eV, and the analyzed area was approximately 2 to 3 mm in diameter. Survey scans (0 to 1200 eV) were collected to determine the elemental species present on the glass surfaces. The compositions of these surfaces were determined from high-resolution scans of the Na KLL, C 1s, O 1s, Al 2p, and Si 2p peaks at a step size of 0.1 eV. The collection time for each peak was adjusted to yield a signal/noise ratio of at least 50/1. Sensitivity factors for the Na KLL, O 1s, Si 2p, and Al 2p peaks were obtained by analyzing the fracture surface of a sodium-aluminosilicate glass (having the molecular formula $\text{Na}_2\text{O}-0.8\text{Al}_2\text{O}_3-2.2\text{SiO}_2$) created in a vacuum of approximately 10^{-6} torr and assuming the atomic percents of

each element on this clean surface matched the bulk composition measured with spectrochemical analysis. The sensitivity factor for the C 1s peak was obtained by analyzing a poly(ethylene terephthalate) film. The surface compositions were expressed as atomic percent ratios normalized to the Si 2p peak. Therefore, the atomic percent ratios reported in this study represent the preferential loss of a given element with respect to Si.

The analysis depth in XPS is a function of the inelastic mean free path of photoelectrons that originate from a given element in the solid and the angle between the analyzer entrance and the sample surface. The depth from which 95% of the signal originates was calculated with the following equation:

$$D = 3\lambda \sin\theta \quad (2)$$

where D is the analysis depth, λ is the inelastic mean free path of a given element, and θ is the angle between the analyzer entrance and a line parallel to the sample surface (i.e., the takeoff angle). The kinetic energies of photoelectrons associated with the Si 2p, Na KLL, and Al 2p peaks are similar in oxide materials and consequently, the inelastic mean free paths and analysis depths are similar (see Seah and Dench, 1979). The average analysis depth for these three elements is approximately 87 Å at $\theta = 65^\circ$ (analysis was not performed at $\theta = 90^\circ$ because of geometric considerations in the Kratos XSAM 800 XPS; tilting the sample to $\theta = 65^\circ$ provided higher count rates and only reduced the analysis depth by 9 Å). It should also be pointed out that XPS averages over the entire analysis depth reported here, so that an analysis depth of 87 Å corresponds to the average composition over the outermost 87 Å of the surface.

2.3.3. SIMS

^1H , ^{16}O , ^{23}Na , ^{27}Al , and ^{29}Si elemental depth profiles of the glass surfaces were obtained with dynamic SIMS with a Cameca IMS/3F spectrometer. A 250 nA, 14.5 keV, $^{18}\text{O}^-$ primary beam was used. A 150- μm -diameter spot was rastered over a 250- \times 250- μm area. Positive secondary ions were collected over a 10- μm -diameter area in the center of the crater. The glass surfaces were not coated; a gold TEM grid provided sufficient surface charge stabilization. Sputtering rates for each of the unreacted glasses were determined by dividing the depth of a sputtered crater (measured with profilometry) by sputtering time. Sputtering rates of all the sodium-aluminosilicate glasses were similar (~ 150 Å/min). Sputtering rates within the leached layers were measured in an analogous manner and found to increase by only 10%.

2.3.4. FTIRRS

FTIRRS spectra of unreacted and reacted glass plates were obtained on a Mattson Research Series spectrometer from 4000 to 400 cm^{-1} with a SiC glow bar source after a 10-min nitrogen purge. Spectra were obtained with 100 coadded scans at an iris opening of 25% and a DTGS detector velocity of 6.2 kHz at 2 cm^{-1} resolution. The interferograms were transformed by use of triangular apodization, and the data were zero filled to increase the spectral point density to 0.5 cm^{-1} . Specular reflectance spectra were obtained with a Spectra-tech attachment. The reflectance spectra were ratioed to the background spectrum of a polished aluminum mirror. These ratioed spectra were then transformed into absorbance spectra by means of a Kramers-Krönig transformation by means of a macro embedded in the WinFirst acquisition software.

3. RESULTS

3.1. Solution Analysis

3.1.1. Dissolution Behavior

Dissolution rates with respect to Si were calculated from the following equation:

$$Q_{\text{Si}} = (C_{\text{Si}}V_{\text{soln}})/(Am) \quad (3)$$

where Q_{Si} is the moles of Si released per square centimeter glass (moles Si/ cm^2), C_{Si} (moles Si/L) is the Si concentration in

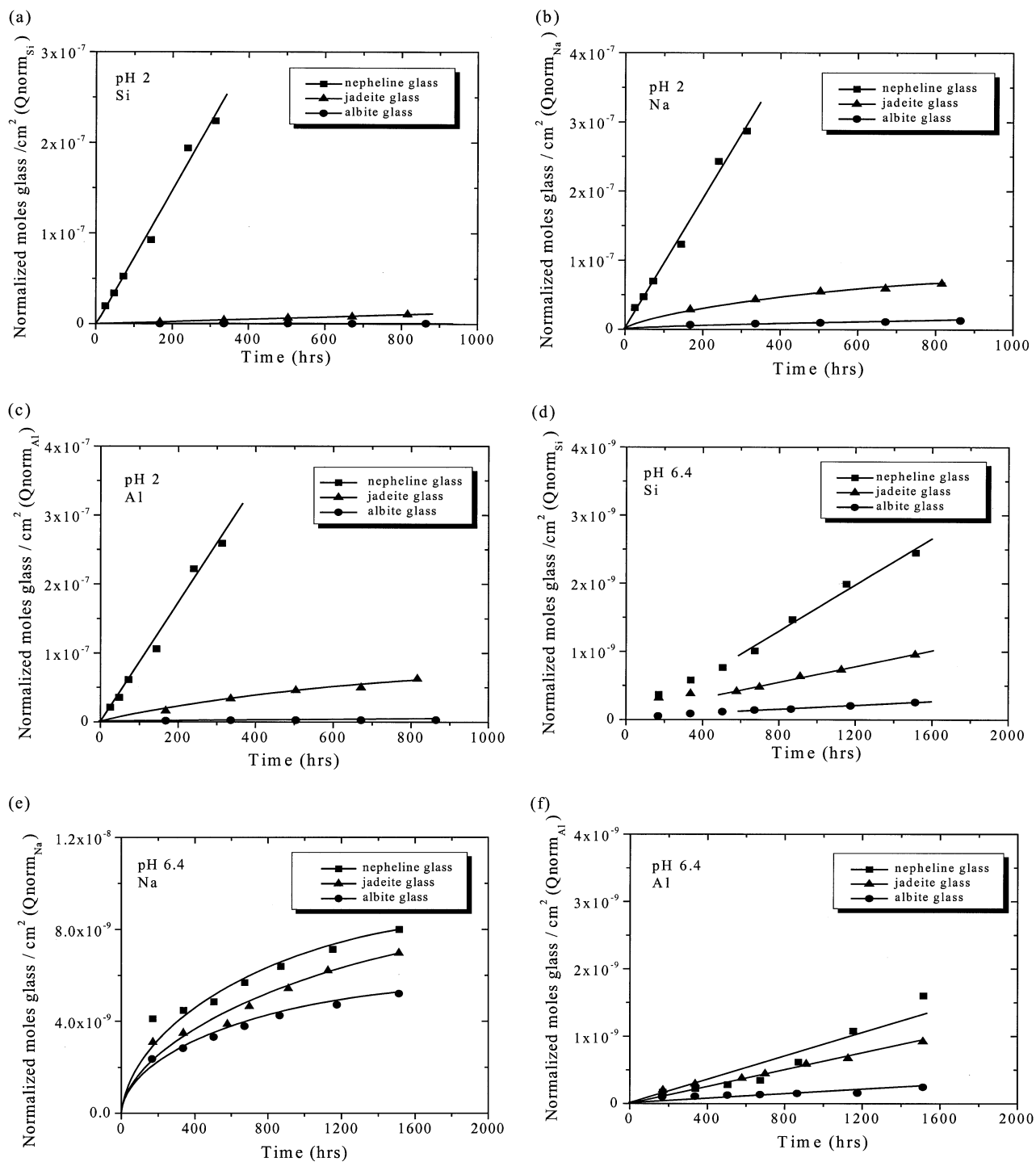


Fig. 2.

solution, V_{soln} (L) is the solution volume (2.300 L), A is the initial specific surface area (cm^2/g), and m is the mass of the glass powder (g). Q_{Si} was assumed to vary with time according to the expression

$$Q_{Si} = k_{dis} t^b \quad (4)$$

where k_{dis} is an apparent dissolution constant, b is an empirical

constant, and t is time (s). Q_{Si} was normalized to the Si concentration in the bulk glass (for a 24 oxygen formula unit: $\text{Na}_{6.01}\text{Al}_{6.01}\text{Si}_{6.01}\text{O}_{24.00}$, $\text{Na}_{4.00}\text{Al}_{4.04}\text{Si}_{7.96}\text{O}_{24.00}$, and $\text{Na}_{3.00}\text{Al}_{3.04}\text{Si}_{8.98}\text{O}_{24.00}$ for nepheline, jadeite, and albite glasses, respectively) to obtain $Q_{norm, Si}$ (moles glass/ cm^2).

Release of Si vs. time (e.g., Fig. 2a, d, g) was initially nonlinear ($b < 1$) for all glasses except nepheline glass reacted

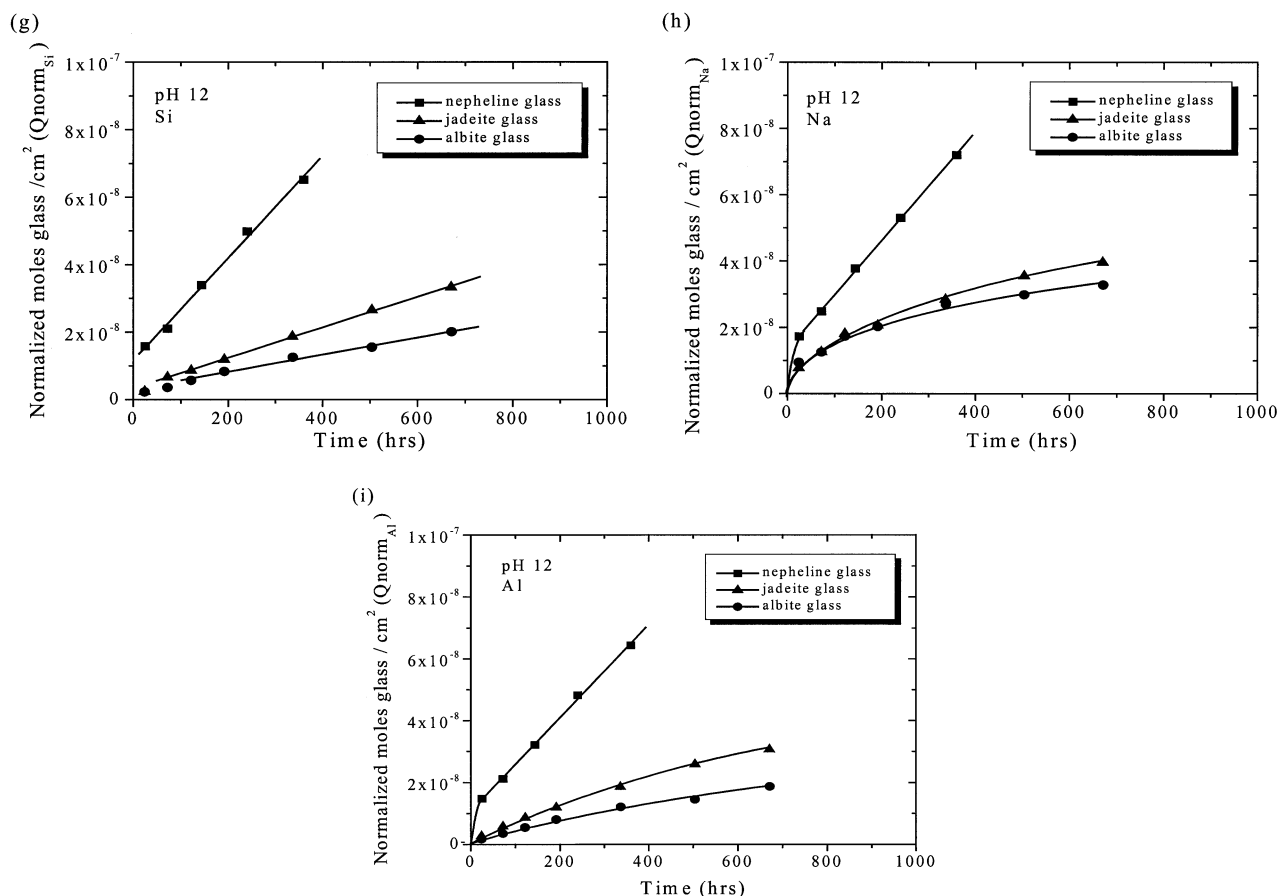


Fig. 2. Normalized concentration with respect to Si ($Q_{norm_{Si}}$) vs. time for the mineral glass powders reacted at (a) pH 2, (d) pH 6.4, and (g) pH 12, 25°C. Normalized concentration with respect to Na ($Q_{norm_{Na}}$) vs. time for the mineral glass powders reacted at (b) pH 2, (e) pH 6.4, and (h) pH 12, 25°C. Normalized concentration with respect to Al ($Q_{norm_{Al}}$) vs. time for the glass powders reacted at (c) pH 2, (f) pH 6.4, and (i) pH 12, 25°C (all glasses are expressed as 24 oxygens per formula unit).

at pH 2. Si release became linear or close to linear with time for all glasses at each pH, but the reaction time required for this transition varied with glass composition and pH. In addition, for nepheline glass dissolution at pH 1, Si release rate decreased between 12 and 24 h, perhaps indicating precipitation of a Si phase. Linear fits to Si release data (by use of only data in the linear portion of the curve) yielded the value of the linear apparent rate constant, k_{dis} (e.g., 2.0×10^{-13} moles glass/cm²/s for nepheline glass reacted at pH 2), for all experiments (Table 2). All such fits yielded R values ≥ 0.940 . By use of the error associated with C_{Si} ($\pm 5\%$, error associated with ICP-AES and ICP-MS measurements) and variability in specific surface area ($\pm 1\sigma$, estimated by repeat measurements with Kr for these low surface area powders as approximately $\pm 35\%$), a conservative estimate of the propagated error in k_{dis} is $\pm 35\%$ ($= (0.05^2 + 0.35^2)^{1/2}$).

Under all conditions, linear apparent rate constants decreased in the order nepheline > jadeite > albite glass (Fig. 3a). As a result of the replacement of Al₂O₃ and Na₂O with 16.3 and 24.8 mol% SiO₂, jadeite and albite glasses dissolved over 300 and 20,000 times slower than nepheline glass, respectively, at pH 1. Dissolution rates of all three mineral glasses decreased to minimal rates near neutral and the rate dependency on pH

decreased at acid pH in the order nepheline > jadeite > albite (Fig. 3b). In contrast to acid dissolution, the pH dependence of dissolution was approximately equal for each glass under basic conditions (Fig. 3c).

3.1.2. Rate Laws and Leaching

Apparent dissolution rate constants, k_{dis} , were fit to the empirical rate law (Table 3),

$$k_{dis} = k_{H^+} (a_{H^+})^{-n} + k_{OH^-} (a_{OH^-})^m \quad (5)$$

where k_{H^+} and k_{OH^-} are the forward rate constants in acid (pH 1 to 4) and base (pH 6.4 to 12), respectively, a_{H^+} is the final activity of protons in solution, a_{OH^-} is the final activity of hydroxyls in solution, and n and m are fit parameters (see Blum and Lasaga, 1988; Hellmann, 1994). In acid, nepheline glass had the highest exponent ($n \sim -1.0$) and albite glass had the lowest exponent ($n \sim -0.2$); in base, the exponents for each glass were approximately equal ($m \sim 0.4$). By fitting rate data to this model, we are implicitly assuming that the activities of Na^+ , Al^{3+} , and Si aqueous species do not measurably affect dissolution, as suggested by generally linear release rates of Si vs. time.

Table 2. Normalized dissolution rates for glass powders.

Glass composition	Initial SSA cm ² /g	Initial pH	Final pH	Log dissolution rate glass (moles Si/cm ² /s)	Log dissolution rate crystal analog (moles Si/cm ² /s)	Log-normalized dissolution rate ^a glass (moles glass/ cm ² /s)
Nepheline	891	1.00	1.21	-10.3 ± 0.1		-11.1 ± 0.1
	891	2.00	2.61	-11.9 ± 0.1		-12.7 ± 0.1
	891	4.00	4.53	-13.5 ± 0.1	-10.3 (pH 3) ^b	-14.3 ± 0.1
	891	6.40	7.03	-14.6 ± 0.1	-12.2 (pH 5) ^b	-15.4 ± 0.1
	891	9.00	9.47	-13.5 ± 0.1	-12.6 (pH 7) ^b	-14.3 ± 0.1
	891	12.00	12.11	-12.4 ± 0.1	-12.6 (pH 11) ^b	-13.2 ± 0.1
Jadeite	644	1.00	1.06	-12.7 ± 0.1		-13.6 ± 0.1
	644	2.00	2.11	-13.5 ± 0.1		-14.4 ± 0.1
	644	4.00	4.10	-14.6 ± 0.1	-12.1 (pH 3) ^c	-15.5 ± 0.1
	644	6.40	6.86	-14.8 ± 0.1	-12.9 (pH 4.6) ^c	-15.7 ± 0.1
	644	9.00	9.27	-14.3 ± 0.1	-12.9 (pH 5.9) ^c	-15.2 ± 0.1
	644	12.00	12.18	-12.9 ± 0.1		-13.8 ± 0.1
Albite	705	1.00	1.04	-14.4 ± 0.1		-15.4 ± 0.1
	705	2.00	2.05	-14.7 ± 0.1		-15.7 ± 0.1
		2.0	2.0	-14.5 ± 0.2 ^d		
	705	4.00	4.12	-15.0 ± 0.1	-14.4 ± 0.2 (pH 2) ^d	-16.0 ± 0.1
		5.6	5.6	-15.7 ± 0.2 ^d		
	705	6.40	6.79	-15.3 ± 0.1	-16.0 ± 0.2 (pH 5.6) ^d	-16.3 ± 0.1
		9.3	8.4	-15.3 ± 0.2 ^d		
	705	9.00	9.68	-14.7 ± 0.1	-15.7 ± 0.2 (pH 8.4) ^d	-15.7 ± 0.1
705	12.00	12.15	-13.0 ± 0.1		-14.0 ± 0.1	

^a Normalized dissolution rates are expressed as mol glass/cm²/s, where all glasses are expressed as 24 oxygens per formula unit (see Table 1).

^b Data from Tole et al. (1986) for batch dissolution of nepheline crystal at noted pH.

^c Data from Sverdrup (1990) for dissolution of jadeite crystal at noted pH.

^d Data from Hamilton et al. (2000) for dissolution in flow reactors of albite glass or crystal as noted, at noted pH.

The quantity of Na and Al released per square centimeter of glass, Q_x (moles x /cm² where $x = \text{Na}$ or Al), was obtained by use of the following equation:

$$Q_x = (C_x V_{\text{soln}})/(Am) \quad (6)$$

where C_x (moles x/L) is the x concentration in solution. Q_{Na} and Q_{Al} were normalized to the Na and Al concentrations in the bulk glass, respectively, to obtain $Q_{\text{norm}_{\text{Na}}}$ and $Q_{\text{norm}_{\text{Al}}}$ (moles glass/cm²) as described previously for Si. Although release of Si was generally observed to be linear with time by the end of each experiment, release of Na and Al was sometimes nonlinear throughout (Fig. 2). Under all conditions, the release of both Na and Al was greatest from nepheline glass (e.g., Figs. 2b, c, e, f, h, i) and lowest from albite glass.

For calculation of the stoichiometry of release, values of Q_{Na} , Q_{Al} , and Q_{Si} were calculated from the Na, Al, and Si concentration data at the completion of the experiments (Table 4). If $Q_{\text{norm}_{\text{Na}}}/Q_{\text{norm}_{\text{Si}}} > 1$, Na was released faster than Si (incongruent dissolution) and either a Si-rich leached layer was formed on the glass surface or a Si-containing precipitate formed. If this ratio = 1, the glass dissolved congruently at the

end of the experiment. If the ratio < 1, Si was released faster than Na and either a Na-rich leached layer was formed or Na-containing precipitation or adsorption reactions may have occurred. We assume that values of these ratios different from unity by more than $\pm \sim 10\%$, where only error in the concentration of solute is considered, indicate lack of congruency. Analogous guidelines apply to describe Al/Si ($Q_{\text{norm}_{\text{Al}}}/Q_{\text{norm}_{\text{Si}}}$) and Na/Al ($Q_{\text{norm}_{\text{Na}}}/Q_{\text{norm}_{\text{Al}}}$) congruency.

For all three glasses, preferential release of Na over Si increased from pH 1 to 6.4 and decreased from pH 6.4 to 12 (Table 4). The extent of Na/Si incongruency decreased in the order albite > jadeite > nepheline glass at all pH values. Release of Na with respect to Si was congruent ($Q_{\text{norm}_{\text{Na}}}/Q_{\text{norm}_{\text{Si}}} = 1.0 \pm 0.1$) for nepheline glass at pH 1 and 12. Release of Al with respect to Si was congruent ($Q_{\text{norm}_{\text{Al}}}/Q_{\text{norm}_{\text{Si}}} = 1.0 \pm 0.1$) for all glasses at pH ≥ 9 . Nepheline glass dissolution was also congruent or only slightly incongruent with respect to Al/Si at pH ≤ 4 . In contrast, Al/Si was highly incongruent from jadeite and albite glasses at pH ≤ 4 (Al/Si $\gg 1$). Al/Si incongruency was greater for jadeite glass than albite glass at pH 1 and 2, but lower at pH 4. At neutral pH,

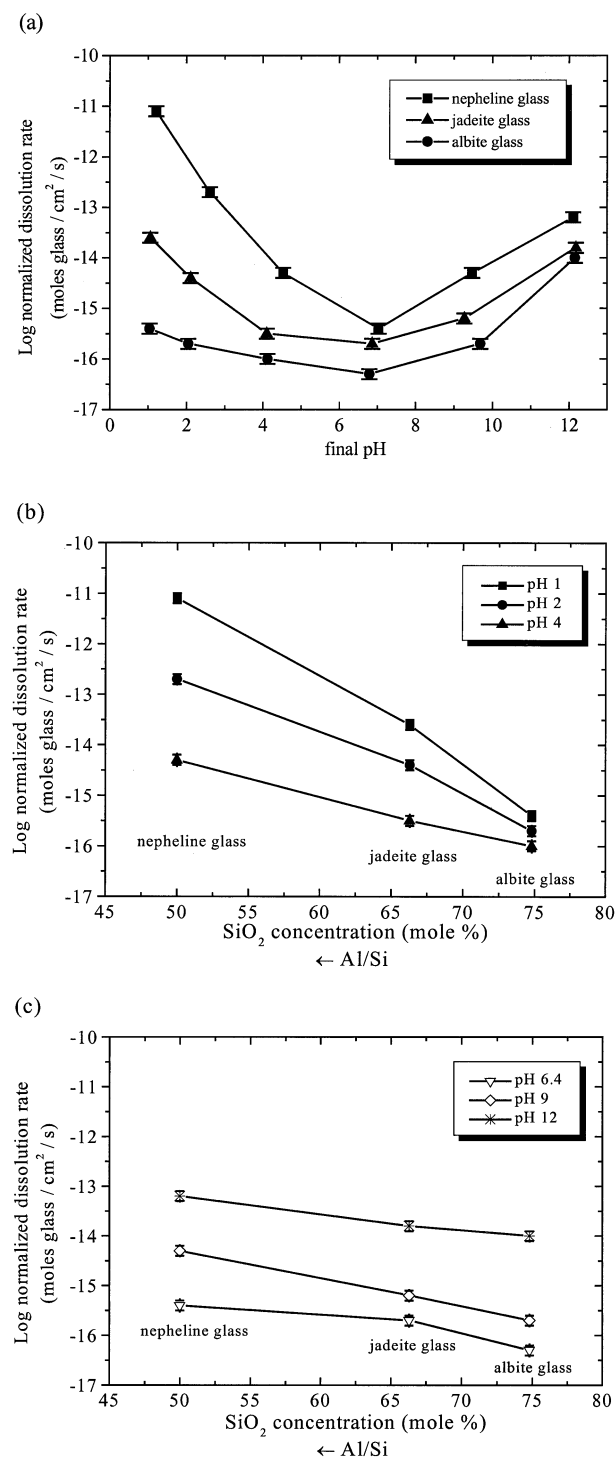


Fig. 3. Normalized dissolution rates with respect to Si vs. (a) pH, (b) SiO₂ concentration at pH ≤ 4, and (c) SiO₂ concentration at pH ≥ 6.4 for the mineral glass powders (all rates expressed as mol glass/cm²/s, where all glasses are expressed as 24 oxygens per formula unit).

dissolution of jadeite and albite glasses was congruent with respect to Al/Si. However, Al/Si < 1 for nepheline glass at neutral pH indicating either the formation of a Al-rich leached layer or Al-containing precipitation or adsorption reactions. For

all three glasses, preferential release of Na over Al increased from pH 1 to 6.4 and decreased from pH 6.4 to 12. The extent of Na/Al incongruity decreased in the order albite > jadeite > nepheline glass at all pH values. Release of Na with respect to Al was congruent ($Q_{norm_{Na}}/Q_{norm_{Al}} = 1.0 \pm 0.1$) for nepheline glass at pH 1, 2, and 12 and jadeite glass at pH 1 and 2.

3.2. Surface Analysis

3.2.1. XPS

The unreacted and reacted surface chemistries (as measured by XPS) and bulk chemistries (as measured by spectrochemical analysis), are presented as Na/Si and Al/Si atomic percent ratios (Fig. 4 and Table 5). The unreacted glass surfaces were slightly altered in both Na and Al compared to their bulk chemistries, presumably because of sample preparation effects. During dissolution, removal of a surface layer should return the surface ratios to the bulk values if dissolution becomes congruent; therefore, atomic ratios between the surface and bulk values are not interpreted to indicate incongruent dissolution. Values more than ~5% above the bulk value or below the surface value are interpreted as documenting incongruent dissolution.

By use of this criteria, Al depletion on nepheline glass was negligible to slight at every pH except 9. In contrast, albite and jadeite glasses showed Al depletion at every pH value except pH 6.4 and 12. Na depletion was significant for every glass at each pH except nepheline glass reacted at pH 1. Both Na and Al depletion were severe on jadeite and albite glasses at pH ≤ 4 but were greatest on jadeite glass. For albite and jadeite glasses, Na depletion decreased (Na/Si increased) as pH increased above 2. In contrast, nepheline glass showed maximum Na depletion at pH 4; as pH increased or decreased, the depletion became less severe.

3.2.2. SIMS

Hydrogen, sodium, and aluminum depth profiles of jadeite glass reacted at pH 2 are illustrated in Figures 5a to c, respectively. The depth of penetration of H and depletion of Na and Al increased throughout the 1100-h treatment at pH 2 (Fig. 5). The sharp interface indicated by the sudden drop in the H/Si ratio and rise in the Na/Si and Al/Si ratios provide excellent markers for the penetration depth of hydrogen into the glass surface and depletion depth of Na and Al from the glass surface. The penetration or depletion depths are defined by the point where the ratio drops by 50% in the interface region. The depth of hydrogen penetration always corresponded exactly to the depth of sodium and aluminum depletion and thus defined the leached layer thickness. The leached layers formed after reaction for 1004 h at pH 1 and 1102 h at pH 2 were both 2100 Å thick.

The H, Na, Al, and Si SIMS depth profiles of jadeite glass reacted at pH 4 to 12 and the albite and nepheline glasses reacted over the entire pH range were identical to the profiles of the unreacted glass surfaces (data not shown), consistent with thin leached layers extending ≤ 200 to 500 Å (which equals the depth sensitivity of SIMS under the experimental conditions) into the surface.

Table 3. Experimentally derived rate laws for glass powders.^a

Composition	n	m	Reference
Nepheline glass	-0.96 ± 0.09	0.43 ± 0.01	This study
Nepheline crystal	-1.0	0.2	Tole et al. (1986)
Jadeite glass	-0.62 ± 0.05	0.36 ± 0.08	This study
Jadeite crystal	-0.70^b		Sverdrup (1990)
Albite glass	-0.19 ± 0.04	0.42 ± 0.14	This study
Albite glass	-0.3	—	Hamilton et al. (2000)
Albite glass	-0.27 ± 0.04^c	0.45 ± 0.12^c	
Albite crystal	-0.5	0.3	Blum and Stillings (1995)

^a Rate = $k_{H^+} (a_{H^+})^{-n} + k_{OH^-} (a_{OH^-})^m$, where solution concentrations are determined by final pH.

^b Sverdrup (1990) calculated this value as a best estimated based on data for jadeite as well as other inosilicates.

^c Based on pH 1, 2, and 4 from this study and 2, 5.6 from Hamilton et al. (2000) (for n) and pH 6.4, 9, and 12 from this study and 5.6 and 9.3 from Hamilton et al. (2000) (for m).

3.2.3. FTIRRS

Absorbance spectra for the unreacted glasses (Fig. 6a) over the 1400- to 400- cm^{-1} range are compared to the FTIRRS spectrum of a sample of unreacted fused silica glass (prepared as described by Guiton, 1991). In the unreacted fused silica glass spectrum, the peak at 1105 cm^{-1} is assigned to antisymmetric stretching vibrations of bridging *SiOSi* bonds within SiO_4 tetrahedra (Sanders et al., 1974; Doremus, 1980; Husung and Doremus, 1990; Roy, 1990). As the SiO_2 concentration decreases in the mineral glass compositions, the *SiOSi* peak gradually shifts to lower wave numbers. Such a shift could be due to perturbation of the *SiOSi* stretching vibration by Al or strongly coupled Al-O and Si-O vibrations (Roy, 1990).

The peak at 808 cm^{-1} in the fused silica glass spectrum is attributed to *SiOSi* symmetric stretching vibrations between SiO_4 tetrahedra (i.e., *SiOSi* bending vibration; Husung and Doremus, 1990). As the SiO_2 concentration decreases in the mineral glasses, this band increases in intensity and shifts to lower wave numbers. This shift may be due to contributions from both Al-O vibrations in the AlO_4^- tetrahedra and Si-O bending vibrations (Roy, 1990). In the nepheline glass struc-

ture, all four apices of the SiO_4 tetrahedra are bonded to AlO_4^- tetrahedra. The peak at 703 cm^{-1} in the nepheline glass spectrum may then be attributed to stretching vibrations between SiO_4 and AlO_4^- tetrahedra (i.e., *AlOSi* stretching vibrations). The lack of a band at $\sim 930 \text{ cm}^{-1}$ indicates a lack of $(\text{AlO}_6)^{3+}$ groups in any of the unreacted glasses (Roy, 1990).

The peak at 467 cm^{-1} in the fused silica glass spectrum is assigned to *SiOSi* and *OSiO* bending vibrations (i.e., *SiOSi* rocking vibration) (Husung and Doremus, 1990). As the SiO_2 concentration decreases in the mineral glasses, this peak shifts to slightly lower wave numbers. Roy (1990) attributes this to the presence of an oxygen linkage to both AlO_4^- and SiO_4 tetrahedra.

The peak positions of each glass reacted for ~ 1000 h over the entire pH range are listed in Table 6. The nepheline and albite glasses reacted at any pH and jadeite glass reacted at pH 4 to 12 exhibited no structural transformation from the unreacted surfaces (e.g., Fig. 6b). The sampling depth in FTIRRS is $> 1 \mu\text{m}$ over the range 1250 to 900 cm^{-1} (Geotti-Bianchini et al., 1991) and therefore, changes in the outer 500Å may not be evident in the absorbance spectra.

Table 4. Normalized concentration ratios for the glass powders.

Glass composition	Final pH	Reaction time (h)	Si concentration 10^{-5} moles/L	Al concentration 10^{-5} moles/L	Na concentration 10^{-5} moles/L	$Q_{\text{norm}_{\text{Na}}}/Q_{\text{norm}_{\text{Si}}}$ ^a		
						$Q_{\text{norm}_{\text{Al}}}/Q_{\text{norm}_{\text{Si}}}$ ^a	$Q_{\text{norm}_{\text{Na}}}/Q_{\text{norm}_{\text{Al}}}$ ^a	
Nepheline glass	1.21	24	452.4	440.9	462.4	1.0	1.0	1.1
	2.61	313	261.2	302.2	334.2	1.3	1.2	1.1
	4.53	531	10.9	12.3	19.1	1.8	1.1	1.5
	7.03	1514	2.85	1.87	9.31	3.2	0.7	4.9
	9.47	1514	32.2	32.0	39.2	1.2	1.0	1.2
	12.11	360	76.0	75.2	84.0	1.1	1.0	1.1
Jadeite glass	1.06	816	61.5	128.5	130.9	4.2	4.1	1.0
	2.11	816	12.2	35.5	37.3	6.1	5.7	1.1
	4.10	864	1.07	0.93	3.91	7.3	1.7	4.3
	6.86	1512	1.07	0.52	3.91	7.3	1.0	7.6
	9.27	1512	2.88	1.56	4.35	3.0	1.1	2.8
	12.18	671	37.2	17.4	22.2	1.2	0.9	1.3
Albite glass	1.04	816	1.60	1.74	5.87	10.9	3.2	3.4
	2.05	864	0.96	1.45	6.09	18.9	4.4	4.3
	4.12	864	0.50	0.48	3.91	23.4	2.9	8.2
	6.79	1512	0.36	0.11	2.39	20.0	1.0	21.1
	9.68	1512	1.60	0.56	2.83	5.3	1.0	5.2
	12.15	672	27.8	8.71	15.1	1.6	0.9	1.8

^a Calculations of $Q_{\text{norm}_{\text{Na}}}$, $Q_{\text{norm}_{\text{Al}}}$ and $Q_{\text{norm}_{\text{Si}}}$ are explained in the text.

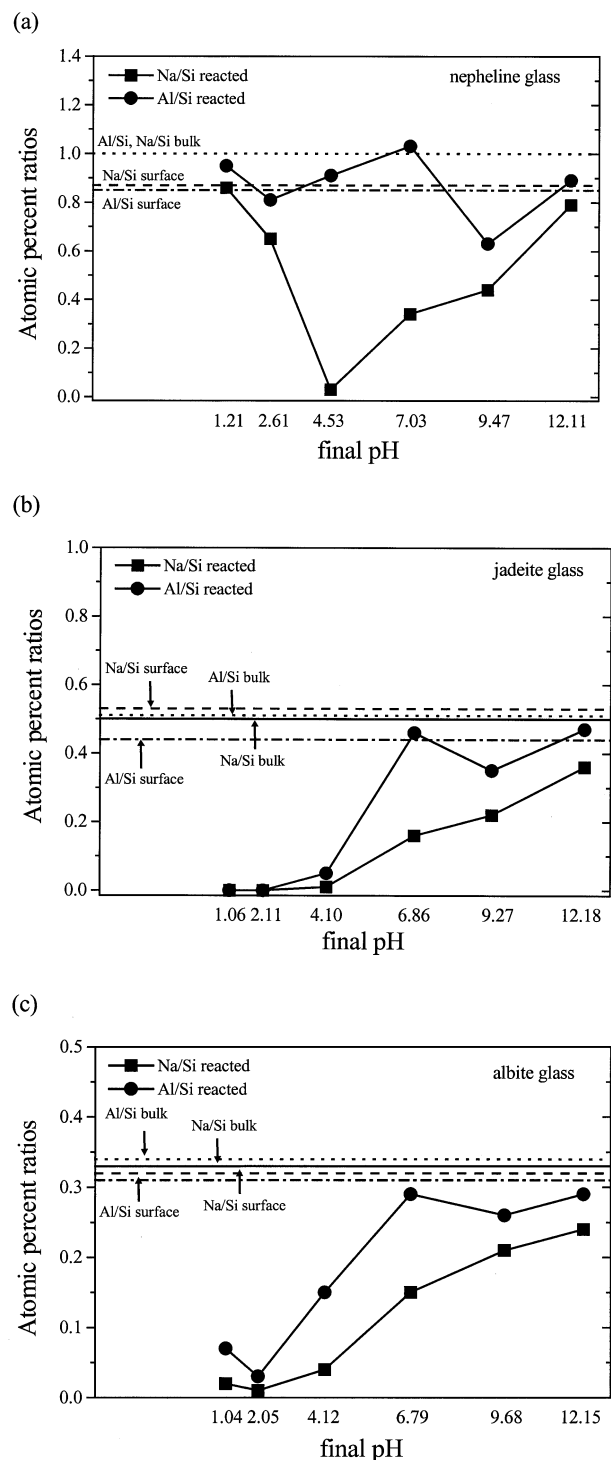


Fig. 4. XPS analyses of (a) nepheline, (b) jadeite, and (c) albite glass plates before (surface) and after reaction in static pH 1 to 12 (see Table 5 for reaction times) solutions at 25°C. Bulk chemistries by spectrochemical analysis (by a lithium metaborate fusion process) are also shown. Error on atomic percent ratios is assumed equal to $\pm 4\%$, following observations summarized by Hamilton et al. (2000).

In agreement with the documentation by SIMS of a ~ 2100 Å thick leached layer, the FTIRRS spectra of jadeite glass reacted in strong acid (pH 1 and 2) indicate transformation of

the near-surface structure (Fig. 6b). This structural transformation is characterized by a shift in the $SiOSi$ stretching vibration from 1029 cm^{-1} in the unreacted glass to 1089 and 1094 cm^{-1} in the glasses reacted at pH 1 and 2, respectively. Also, broad bands at 1003 and 990 cm^{-1} appear in the reacted glass spectra that are probably due to Si-O vibrations coupled with Al-O vibrations in the bulk glass only. The structure of the leached layer that forms on the jadeite glass surface during reaction in acid is somewhat similar to the structure of an acid-catalyzed xerogel (i.e., very open, porous, and weakly cross-linked according to Guillon, 1993) as evidenced by similarities in the peak positions of the $SiOSi$ stretching vibrations (Fig. 6b).

4. DISCUSSION

4.1. Comparison to Published Dissolution Rates

Several lines of evidence suggest that Si release rates in Table 2 are excellent indicators of trends in dissolution for these glasses. For example, the three glasses clearly show a minimum in dissolution rate at near-neutral pH like plagioclase feldspars (Blum and Stillings, 1995) and glasses along the sodium disilicate–nepheline, $Na_2O-xAl_2O_3-2SiO_2$, and other joins (investigated primarily at 40°C for up to 12 h; Dubrovo and Schmidt, 1953, 1955a,b; Dubrovo, 1954a,b, 1958; Schmidt, 1954a,b). Consistent with observations for plagioclase crystals, dissolution rates increase with increasing Al content (albite < jadeite < nepheline glass) at all values of pH (Fig. 3). Furthermore, Hamilton et al. (2000) report a $\log(\text{rate (mol Si cm}^{-2}\text{ s}^{-1)})$ measured in a flow reactor for albite glass at pH 2 of -14.5 ± 0.2 , within error of the rate measured here (Table 2). Finally, given that Hamilton et al. (2000) reported that albite glass and crystal dissolution rates were indistinguishable, we can also compare glass dissolution here to rates for similar crystals in the literature. For example, the value of n reported for crystal and glass of nepheline and jadeite composition and m for crystal and glass of albite composition are indistinguishable within error (Table 3).

A few discrepancies among glass and crystal dissolution rates are apparent in comparing Tables 2 and 3 to literature values. The value of m reported here for nepheline glass is about a factor of two smaller than that reported in the literature for nepheline crystal (Table 3). In addition, dissolution rates reported for nepheline crystal (Tole et al., 1986) are consistently higher than rates measured for the glass (Table 2). However, these discrepancies may be explained by the higher K content of the nepheline crystal used by Tole et al. as compared to the glass ($K/Na_{\text{crystal}} = 0.25$). The faster dissolution rates measured by Sverdrup (1990) for jadeite crystal as compared to the jadeite glass here may be related to the difference in structure between the glass and crystal: the chains of silica tetrahedra released after leaching of Al from the crystal may be hydrolyzed into solution at a faster rate than the partially interconnected silica tetrahedra left after aluminum leaching of the glass.

Data reported here show many similarities to aqueous corrosion of glass as reported over the past several decades (see Bacon, 1968; Clark et al., 1979; Clark and Zoitos, 1992; Doremus, 1994). In general, dissolution of alkali–aluminosilicate glasses has been modeled as a combination of diffusion-controlled extraction of alkali ions occurring with break down

Table 5. XPS and SIMS analyses of unreacted and reacted glass plates.

Glass composition	Final pH	Reaction time (h)	XPS Na/Si	XPS Al/Si	SIMS hydrogen penetration depth
Nepheline glass		Bulk chemistry ^a	1.00	1.00	
		Unreacted surface chemistry ^b	0.87	0.85	
	1.11	100	0.86	0.95	≤200–500 Å
	2.16	1004	0.65	0.81	≤200–500 Å
	4.40	1057	0.03	0.91	≤200–500 Å
	7.09	1000	0.34	1.03	≤200–500 Å
	9.20	1004	0.44	0.63	≤200–500 Å
	12.09	1005	0.79	0.89	≤200–500 Å
Jadeite glass		Bulk chemistry ^a	0.50	0.51	
		Unreacted surface chemistry ^b	0.53	0.44	
	1.00	1004	0.00	0.00	2100 Å
	2.03	1102	0.00	0.00	2100 Å
	4.04	1000	0.01	0.05	≤200–500 Å
	6.59	1002	0.16	0.46	≤200–500 Å
	8.40	1102	0.22	0.35	≤200–500 Å
	12.06	1007	0.36	0.47	≤200–500 Å
Albite glass		Bulk chemistry ^a	0.33	0.34	
		Unreacted surface chemistry ^b	0.32	0.31	
	1.00	1009	0.02	0.07	≤200–500 Å
	2.04	1000	0.01	0.03	≤200–500 Å
	3.98	1010	0.04	0.15	≤200–500 Å
	7.18	1010	0.15	0.29	≤200–500 Å
	9.16	1000	0.21	0.26	≤200–500 Å
	12.06	1009	0.24	0.29	≤200–500 Å

^a Bulk chemistry is based on a lithium metaborate fusion process followed by ICP-AES analysis of the resulting solution.

^b Unreacted surface chemistry based on XPS analysis of glass plate surfaces after polishing, cleaning, and etching procedures as described in text.

of silicate matrix (see Grambow, 1992; White, 1992; Doremus, 1994, for reviews). In sodium–aluminosilicate glasses with Al/Na ratio = 1, such as the mineral glasses studied here, no nonbridging oxygens are present and Na⁺ ions are associated with AlO₄ tetrahedra (Brückner et al., 1978; Shelby, 1978; Smets and Lommen, 1981; Onorato et al., 1985; Goldman, 1986; Hsieh et al., 1994). Smets and Lommen (1982) proposed that such Na⁺ ions are leached by interdiffusion of hydrogen (or hydronium) and alkali ions (Doremus, 1975). Hench and Clark (1978) pointed out that the addition of alumina to sodium–silicate glasses significantly reduces the rate of selective Na leaching and promotes the formation of protective films through structural changes in the glass surface, precipitation from solution, or both.

It has generally been reported that the initial rate of ion exchange on glass surfaces obeys parabolic kinetics, but at later stages, alkali release becomes linear with respect to time, as release is controlled by network breakdown (see Doremus, 1994, for a review). In the initial stages of alkali–silicate glass dissolution, alkali release is controlled by diffusion across the leached layer from the bulk glass into solution. As leached layer thickness increases with time, the diffusion process gradually slows down until the alkali release rate becomes equivalent to the Si release rate from the leached layer/solution interface (Douglas and El-Shamy, 1967). At this point, the velocity of the leaching front is equivalent to the velocity of the dissolution front, leached layer thickness is constant, and steady-state dissolution is achieved. Release of silica to solution has also been commonly observed to be nonlinear at short

reaction times but rapidly becomes linear with time. This initial nonlinear release of Si may be attributed to enhanced surface strain or high surface area features such as surface fines or microcracks induced by grinding, or to the time-dependent establishment of a steady-state leached layer (see Eggleston et al., 1989; El-Shamy et al., 1972). Consistent with these published observations, albite, jadeite, and nepheline glasses were generally observed to release Na, Al, and Si nonlinearly in the initial stages of reaction (Fig. 2). However, Si release was generally observed to become linear with time well before the end of each experiment (the time until linear release was achieved varied with solution pH and glass composition). In contrast, Na and Al release did not always become linear with time by the end of each experiment. The lack of linear release of these last two components in our experiments may indicate that the experiments did not reach steady state. Indeed, Melnyk et al. (1983) report that dissolution of Sr- and Cs-doped nepheline syenite–based glass spheres release Sr and Cs at decreasing rates even after 2400 h of dissolution at near-neutral pH.

Other evidence may also imply that dissolution did not reach steady state for at least a few of the batch albite glass runs. The value of n (-0.19 ± 0.04) measured for albite glass dissolution below pH 5 here (Table 3) is lower than would be calculated from dissolution rates measured at pH 2.0 and 5.6 for albite glass reported in our earlier work ($n = -0.3$; Hamilton et al., 2000). Hamilton et al. (2000) report that approximately 1000 h is needed to reach steady-state dissolution for albite glass at pH 2; in contrast, longer durations are needed at pH 5.6 and 8.4 (3500 and 3000 h, respectively). Given that the length of time

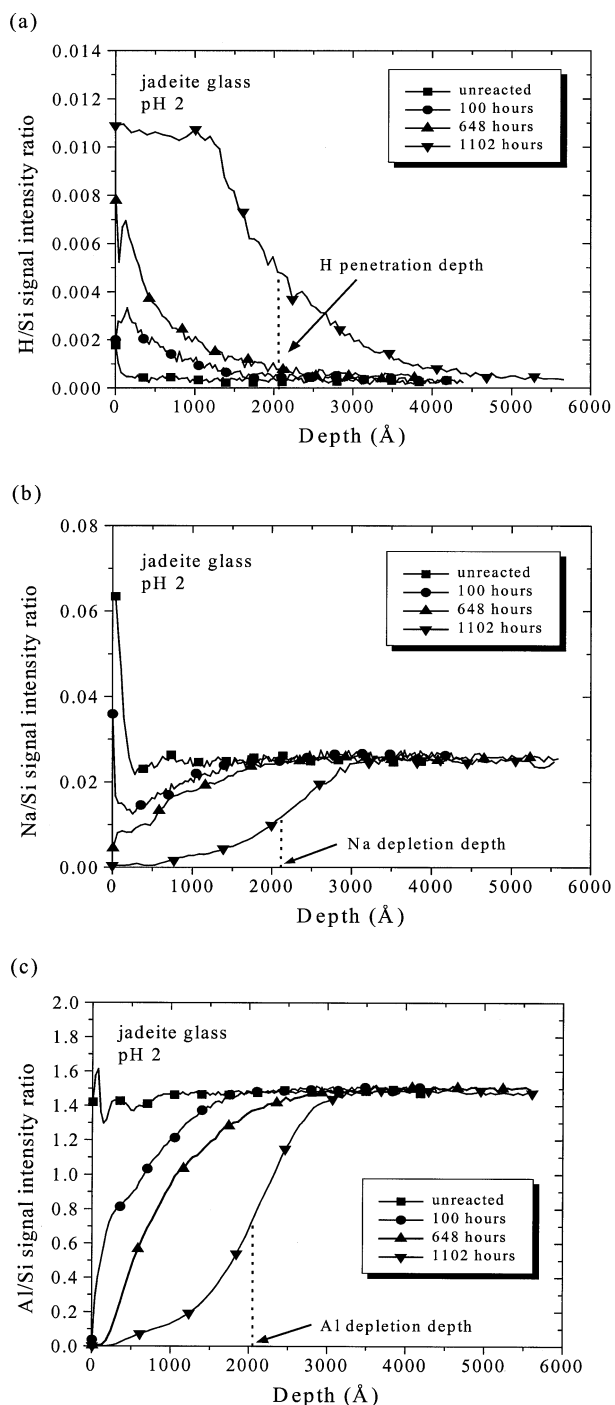


Fig. 5. SIMS (a) hydrogen, (b) sodium, and (c) aluminum depth profiles of jadeite glass plates reacted in static pH 2 solution at 25°C. Profiles are plotted as the H/Si, Na/Si, or Al/Si secondary intensity ratio on the ordinate vs. depth on the abscissa.

to reach steady-state correlates with the rate of dissolution (Hamilton et al., 2000), steady state may only be assumed for albite experiments here with $\log(\text{dissolution rates}) > -14.7$ (the rate of albite glass dissolution where rates measured here and by Hamilton et al. are consistent). Rates of dissolution for albite glass at pH 4 to 7 may not have reached steady state.

Following from this, the value of n must be ≤ -0.19 and $m \geq 0.42$ for albite glass. Perhaps a better estimate of n can be obtained by recalculating with rates measured here together with data from Hamilton et al. (2000): $n = -0.27 \pm 0.04$. This value differs from the value reported in a recent review (-0.5) but within the range of reported values in the literature for albite crystal (-0.2 to -0.5 , Blum and Stillings, 1995). Without better control on the value of n for albite glass, it remains unclear whether the value of this parameter is identical or different between glass and crystal.

4.2. Leaching Behavior and Surface Layer Structure

Solution chemistry (Table 4) is generally consistent with observations from XPS (Fig. 4, Table 5) in indicating congruent or incongruent dissolution. In general, both solution and XPS data taken together indicate little to no Al depletion from any of the glasses dissolved at high pH nor from nepheline glass at low pH. However, by use of data from Stumm and Morgan (1996), gibbsite is calculated to be supersaturated at pH 6 and 9 for every experiment. In fact, for every phase, XPS results suggest relatively high Al/Si surface ratios at pH 6.4, perhaps documenting some Al back-precipitation onto the surface at this pH. Supersaturation with respect to amorphous silica was also calculated to have occurred at pH 1 and 2 during nepheline glass dissolution. Consistent with this, the dissolution rate for nepheline glass decreased between 12 and 24 h for pH 1 (this inferred precipitation explains why the nepheline experiment was terminated at 24 h at pH 1). No evidence for precipitation was observed in Si release rates with time for nepheline glass at pH 2. Furthermore, precipitation of Si was not documented by XPS (higher Si/Al ratios); a precipitate was not documented by scanning electron microscopy (performed on plates or powders) or documented by X-ray diffraction (performed on powders) for any phases reacted at any pH. In contrast to the Al/Si congruency, solution and XPS data document that Na/Si incongruity increases above pH 1 and then decreases for dissolution of nepheline glass above pH 6.4. Both solution and XPS data also show Na depletion on albite and jadeite glasses for most values of pH, and especially at low pH.

These observations can be compared to literature reports for some glass compositional systems. The corrosion behavior of glasses along the sodium disilicate–nepheline, $\text{Na}_2\text{O}-x\text{Al}_2\text{O}_3-2\text{SiO}_2$, and other joins was investigated primarily at 40°C for up to 12 h (Dubrovo and Shmidt, 1953, 1955a,b; Dubrovo, 1954a,b, 1958; Shmidt, 1954a,b). Similar to our observations, the nepheline composition (Al/Si = 1) dissolved congruently at pH 1. Also similar to our observations, dissolution rates for disilicate–nepheline glasses were always slower at neutral and faster at acid and basic pH values. However, Dubrovo (1954a), Shmidt (1954b), and Dubrovo and Shmidt (1955a) have shown that release rates of Na, Al, and Si from sodium disilicate glasses are either inhibited or enhanced by changes in x over the range of $x = 0$ to 1.0 for glass compositions with the general formula $\text{Na}_2\text{O}-x\text{Al}_2\text{O}_3-2\text{SiO}_2$, depending upon whether solutions are acid (0.1 N HCl), neutral (water), or basic (0.1 N NaOH). For example, dissolution of glass along the sodium disilicate–nepheline join with $x = 0.3$ under acidic conditions created Al-depleted surface layers. In contrast, for glasses with $x > 0.5$, the residual surface layer was enriched in Al after

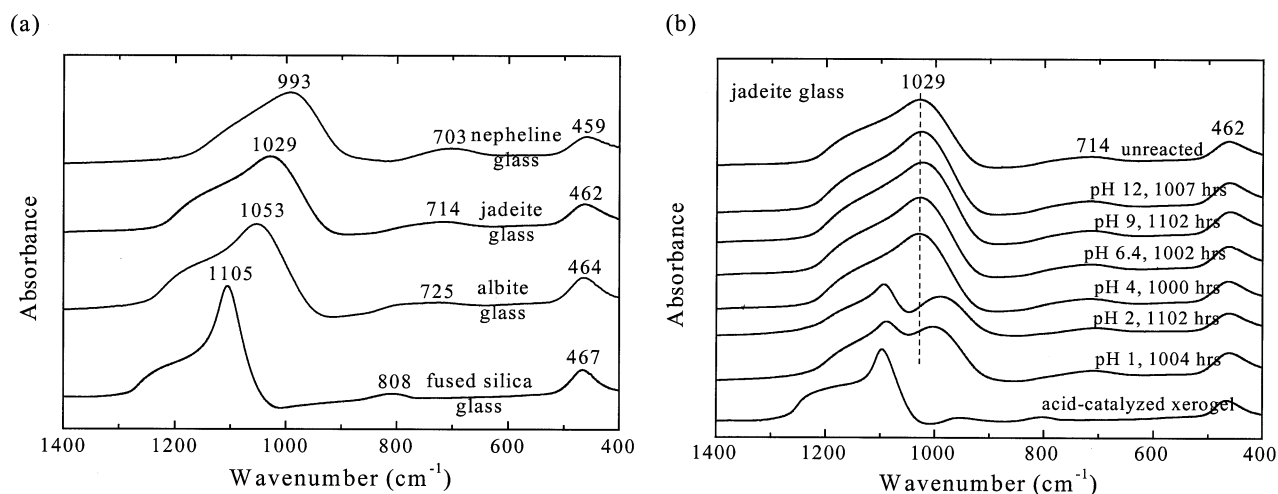


Fig. 6. Absorbance spectra of (a) unreacted nepheline, jadeite, albite, and fused silica glass plates and (b) jadeite glass plates after reaction in static pH 1 to 12 solutions at 25°C. Spectra are offset to highlight changes in peak position and shape.

dissolution under neutral conditions. Al enrichment was attributed to adsorption of Al species onto the glass surface. In this suite of glasses, alumina replaces both silica and soda in the sodium disilicate composition. Similar observations of both decreases and increases in Na, Al, and Si release rates of sodium trisilicate glasses ($\text{Na}_2\text{O}-x\text{Al}_2\text{O}_3-(3-x)\text{SiO}_2$ with values of x from 0 to 1.0) were reported by Kerly (1983) at pH 7.2 and temperatures between 30 and 90°C. In this suite of glasses, alumina replaced silica in a sodium-trisilicate composition with constant soda content. Interpretation of some of these reported observations is difficult because of lack of detail about experiments and analytical techniques, and the short times used for dissolution.

The hydrogen profiles that we collected on our three glasses document that all leached layers were ≤ 200 to 500 Å except for jadeite glass leached in strong acid. The thicker leached layer on jadeite glass reacted at pH ~ 2 revealed FTIR spectra consistent with a porous, gel-type structure similar to that of an acid-catalyzed xerogel (Fig. 6b). The structure of an acid-catalyzed xerogel is very open, porous, and weakly cross-linked (Guiton, 1993). The SIMS data for jadeite glass dissolved at pH 2 documents interdiffusion profiles of Na, Al, and H (see, for example, interdiffusion profiles as calculated by Hellmann (1997) for albite reacted in aqueous solutions). The structure of the thin leached layer formed on albite in acid may have a similar gel-type structure (see also Hamilton et al.,

Table 6. Peak positions and assignments of Kramers-Krönig transformed absorbance spectra.

Glass composition	Final pH	Reaction time (h)	Si-O-Si stretch	Si-(OAl) stretch	Si-O stretch	Si-O-Si bend	Si-O-Si rock
Acid-catalyzed xerogel ^a			1097		954	803	467
Fused silica glass ^a			1105			808	467
Nepheline glass		Unreacted	993			703	459
	1.11	100	994			705	460
	2.16	1004	995			702	459
	4.40	1057	993			702	458
	7.09	1000	995			703	459
	9.20	1004	992			704	458
	12.09	1005	994			702	459
Jadeite glass		Unreacted	1029			714	462
	1.00	1004	1089	1003		708	461
	2.03	1102	1094	990		704	461
	4.04	1000	1023			715	460
	6.59	1002	1027			714	463
	8.40	1102	1029			716	463
	12.06	1007	1026			715	460
Albite glass		Unreacted	1053			725	464
	1.00	1009	1049			718	462
	2.04	1000	1056			719	462
	3.98	1010	1051			722	462
	7.18	1010	1053			722	463
	9.16	1000	1050			725	462
	12.06	1009	1051			722	463

^a From Guiton (1991, 1993).

2000) although this could not be measured with FTIRRS because of the analysis depth of this technique ($>1 \mu\text{m}$ at 1250 to 900 cm^{-1}).

The thickness of the altered layer formed on surfaces of plagioclase feldspars during dissolution at pH 3.5 measured with SIMS and XPS by Muir et al. (1990) also varied as a function of Al/Si ratio. Like the transition from jadeite (Al/Si = 0.5) to albite (Al/Si = 0.3) glass, labradorite (Al/Si = 0.66 to 0.8) and bytownite (Al/Si = 0.8 to 0.9) crystals had much thicker altered layers than albite (Al/Si < 0.4), oligoclase (Al/Si = 0.4 to 0.5) and andesine (Al/Si = 0.5 to 0.66) crystals. In addition, like nepheline glass (Al/Si = 1.0), dissolution of anorthite (Al/Si = 1.0) is almost stoichiometric with respect to Al at low pH (Amrhein and Suarez, 1988). For both plagioclase and the albite–jadeite–nepheline series, then, as Al/Si increases from 0.3 to 1.0, Al-leaching increases to some point above which value the mineral dissolves rapidly and stoichiometrically without formation of a leached layer. This threshold Al/Si value is ≥ 0.5 for the mineral glasses and ≥ 0.9 for plagioclase. In contrast to this evidence for Al-depletion at low pH on plagioclase, little to no evidence exists in the literature for Al leaching on plagioclase at high pH—again consistent with results observed here for the mineral glasses (see Hamilton et al., 2000, for a discussion of data for albite).

4.3. Mechanisms of Dissolution

Grambow (1992) suggests that dissolution of an aluminosilicate glass is rate limited by hydrolysis of an activated surface complex ($-\text{Si}(\text{OH})_3$) within a reacted surface zone. This model is similar to models that describe crystalline feldspar dissolution rates by reactions at and within altered surface layers (e.g., Helgeson et al., 1984; Blum and Lasaga, 1988, 1991; Murphey and Helgeson, 1984; Wieland et al., 1988; Schott, 1990; Hellmann, 1995; Brantley and Stillings, 1996, 1997). However, the nature of such sites have not been well characterized, as such layers must contain atoms in varying states of connectivity (Hellmann et al., 1990). Such sites most likely consist of terminal OH groups (silanol or aluminol) or bridging oxygens (AlOSi or SiOSi linkages).

At high pH, Brady and Walther (1992) and Blum and Lasaga (1991) hypothesized that deprotonation of terminal Si or Al sites respectively controls dissolution. Brady and Walther (1992) suggested that m should equal 0.3 for all (alumino)silicates at high pH. Values of m for two of the three glasses studied here are within error of this predicted value (Table 3). Consistent with this model, the ab initio calculations of Kubicki et al. (1996) show that deprotonation of terminal Si groups weaken the bonds connecting the group to the mineral. Alternately, another mechanism suggested for borosilicate glasses (Bunker et al., 1988), nucleophilic attack of Si sites by OH^- to form five-coordinate Si transition states could also occur (Kubicki et al., 1993). Given the observation that little to no Al depletion occurs on the mineral glasses dissolved at high pH in this work, our observations are consistent with a mechanism for dissolution at high pH of either hydrolysis of deprotonated silanol groups (e.g., Brady and Walther, 1992), or nucleophilic attack by OH^- at Si sites.

In contrast to high pH dissolution, most aluminosilicates develop an Al-depleted layer at low pH. Schott (1990), Blum

and Lasaga (1991), Brady and Walther (1992), and Walther (1996, 1997) suggested that protonation of terminal Al hydroxyl sites within the hydrated layer of feldspars controls dissolution at low pH. However, calculations by Kubicki et al. (1996) suggest that protonation of terminal Al groups should strengthen rather than weaken the connecting bonds to the underlying mineral. Instead of simple surface protonation of silanol or aluminol groups, Hellmann (1995) suggested a “leached layer-surface reaction” model in which the dissolution rate of feldspar (albite) is viewed as a 3D rather than 2D process controlled by detachment of Si influenced by exchange, hydrolysis, and condensation occurring within leached layers. If reactions within the leached layer control dissolution, and if the mechanisms of dissolution of all three glasses studied here are identical as suggested by smooth variation in dissolution behavior with Al content, this is consistent with a mechanism wherein hydrolysis of fully connected Si and Al tetrahedra are rate controlling (see earlier discussion by Brantley and Stillings, 1996, 1997).

For this discussion, we note Al and Si atoms bonded to v bridging oxygens as Q_v^{Al} and Q_v^{Si} , respectively. Hydrolysis of the bridging oxygen between two Q_4 sites is a “network-opening” reaction at the leached layer-bulk mineral interface. This reaction is followed by hydrolysis of Q_3 to Q_2 to Q_1 until release of the aqueous complex (Hellmann et al., 1990). Indeed, Hellmann et al. (1990) noted that the Q_3 , Q_2 , and Q_1 sites are equivalent to layer, edge, and adatom sites, respectively. As sequential reactions, the slowest of these hydrolysis steps should control dissolution. Brantley and Stillings (1997) argued that the rate of hydrolysis of Q_4Q_4 is slower than those for Q_3 to Q_2 and Q_1 , and thus should be rate controlling. This prediction is consistent with observations made by Bunker et al. (1988) for other glass compositions and with recent calculations (Pelmenschikov et al., 2000) showing that the higher the connectivity of an Si atom, the stronger the resistance to breaking the SiOSi bond.

As long as every tetrahedron has four bridging oxygens and at least one AlOSi linkage, then network opening will occur by hydrolysis of bridging oxygens between Q_4^{Al} and Q_4^{Si} or between Q_4^{Si} and Q_4^{Si} . At low pH, Brand et al. (1993), Sykes and Kubicki (1993), and Xiao and Lasaga (1995) use ab initio calculations to argue that protonation of the AlOSi bridging oxygen significantly weakens the bridging bond and that hydrolysis of AlOSi is faster than SiOSi (see also discussions in Geisinger et al., 1985, and Hellmann et al., 1990). On the basis of such calculations and on the basis of the observation that Al is released faster than Si at low pH, it is assumed that hydrolysis of $Q_4^{\text{Al}}Q_4^{\text{Si}}$ dominates network opening. Once network opening has occurred, hydrolysis of Q_3^{Al} to Q_2^{Al} to Q_1^{Al} to Q_0^{Al} must occur faster than Q_3^{Si} to Q_2^{Si} to Q_1^{Si} to Q_0^{Si} in order that Al be released faster than Si (e.g., Hellmann et al., 1990), as observed for all phases with Al/Si < 1 at low pH. However, two possibilities remain: either the hydrolysis of $Q_4^{\text{Al}}Q_4^{\text{Si}}$ is faster or slower than hydrolysis of Q_3^{Si} to Q_2^{Si} to Q_1^{Si} to Q_0^{Si} .

If hydrolysis of $Q_4^{\text{Al}}Q_4^{\text{Si}}$ is slower than hydrolysis of Q_v^{Si} ($v < 4$), then hydrolysis of $Q_4^{\text{Al}}Q_4^{\text{Si}}$ should rate limit dissolution at subneutral pH for these glasses. The importance of hydrolysis of the AlOSi bond has been emphasized by previous workers (e.g., Hellmann et al., 1990; Oxburgh et al., 1994; Xiao and Lasaga, 1995). By assuming a random distribution of AlO_4^-

tetrahedra, the number of $AlOSi$ linkages per SiO_4 tetrahedron can be calculated from bulk chemistry to be equal to 4 times the Al/Si ratio in a phase. For example, albite glass contains 7.8 Al/23.0 Si atoms (1.36 $AlOSi$ per SiO_4 tetrahedron). By use of this procedure, jadeite and nepheline glasses contain 2.03 and 4.00 $AlOSi$ linkages per SiO_4 tetrahedron, respectively. Consistent with these values, albite, jadeite and nepheline glass contain 2.64, 1.97 and 0 $SiOSi$ linkages per SiO_4 tetrahedron, respectively (Table 1).

If network opening (hydrolysis of Q_4 species) is rate limiting, two inconsistencies remain. In order for removal of Al from the surface to leave a Si-rich leached layer on jadeite and albite, the rates of hydrolysis of $Q_v^Si Q_w^Si$ ($v, w \leq 3$) must not be much faster than network opening, suggesting some kind of multiple step control on dissolution. Furthermore, if network opening is rate limiting, we might expect that rates of dissolution of the three glasses studied here would be identical (but compare Fig. 3). Ab initio calculations were therefore performed on molecules believed to be representative of the structures in these glasses to elucidate the effect of composition on dissolution mechanisms. Calculations were performed with Gaussian 98 (Frisch et al., 1998). Geometry optimizations for each molecule were calculated by means of self-consistent, Hartree-Fock molecular orbital calculations with a 3-21G** basis set. Figure 7a illustrates the optimized geometry of a $Q_4Si(AlNa)$ molecule (Sykes et al., 1997): the notation refers to a central SiO_4 tetrahedron bonded to 1 AlO_4^- tetrahedron charge compensated by a Na^+ , and 3 other SiO_4 tetrahedra. The $Q_4Si(AlNa)$ molecules represent the primary structural units present in albite glass. The $Q_4Si(2Al,2Na)$ molecule (Fig. 7b) represents the primary structural unit present in jadeite glass. Finally, the $Q_4Si(4Al,4Na)$ molecule (Fig. 7c) represents the primary structural units present in nepheline glass.

It is evident from the simulated molecules that replacement of Si atoms with Al atoms in the glass structure causes an increase in the average Si-O bond length within $SiOAl$ linkages. Furthermore, the average Si-O bond length within $SiOSi$ linkages ($\sim 1.64 \text{ \AA}$) and the average Al-O bond length within $AlOSi$ linkages ($\sim 1.77 \text{ \AA}$) do not change as Al is added to the network. The average bond length of Si-O bonds within $AlOSi$ linkages increases from $\sim 1.58 \text{ \AA}$ in albite glass to $\sim 1.60 \text{ \AA}$ in jadeite glass to $\sim 1.62 \text{ \AA}$ in nepheline glass. Lengthening of this bond suggests that hydrolysis of $AlOSi$ bonds may become energetically more favorable as the number of AlO_4^- tetrahedra per central SiO_4 tetrahedron increases. In other words, nepheline glass should hydrolyze more rapidly than jadeite glass and albite glass, as observed.

This model assumes that hydrolysis of a bridging oxygen between Q_4^Al and Q_4^Si is slightly faster than between Q_v^Si and Q_w^Si ($v, w \leq 3$). If this assumption is untrue, then the rate-limiting step of dissolution for albite and jadeite might not be network opening but might instead be hydrolysis of $Q_v^Si Q_w^Si$ ($v, w \leq 3$). If all Al were leached from the glass surface, the rate-limiting hydrolysis reaction might then vary from one glass to the next: for example, hydrolysis of $Q_3^Si Q_3^Si$, $Q_2^Si Q_2^Si$, and either $Q_4^Si Q_4^Al$ or $Q_3^Si Q_3^Al$ would rate limit albite, jadeite, and nepheline dissolution, respectively. In contrast, if much Al were retained in the leached layer, the mechanism of dissolution might not depend on composition for phases with Al/Si < 1 , as predicted by the models of Oelkers et al. (1994) and Oelkers and Schott (1995):

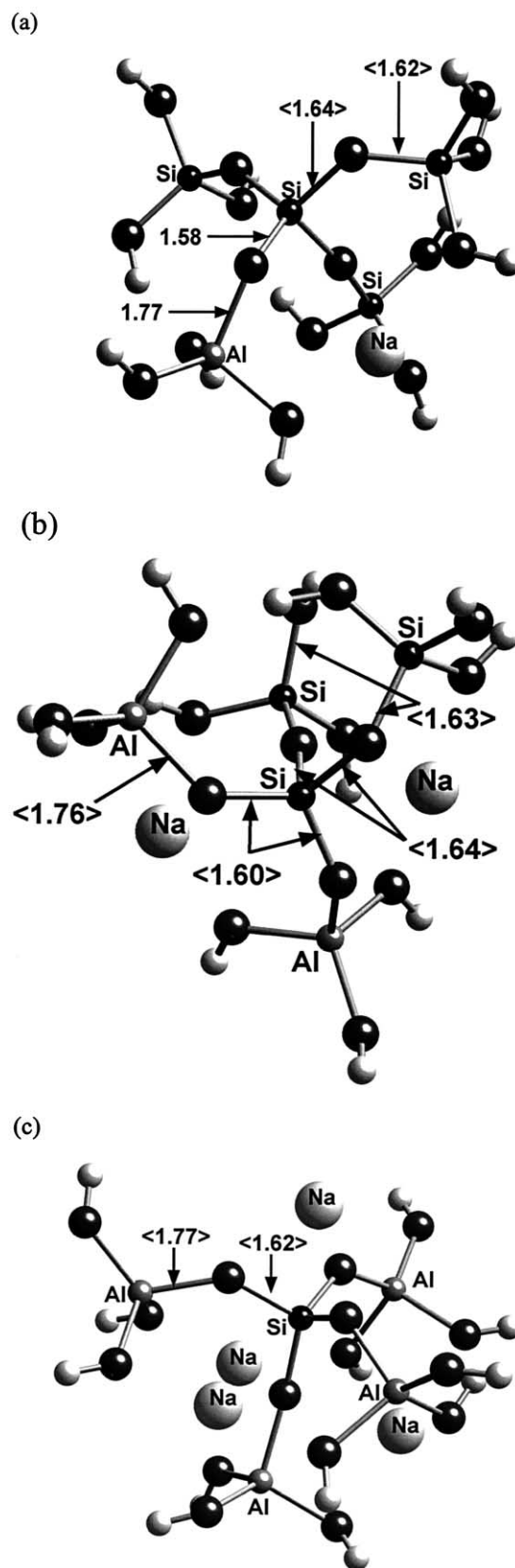


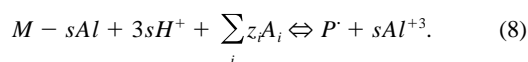
Fig. 7. Optimized geometries (HF/3-21G**) of the (a) $Q_4Si(AlNa)$, (b) $Q_4Si(2Al,2Na)$, and (c) $Q_4Si(4Al,4Na)$ molecules. The bond lengths in brackets are average values.

these models implicitly assume that hydrolysis of $Q_2^Si Q_2^S$ and $Q_3^Si Q_3^{Al}$ rate limits dissolution of albite/jadeite and nepheline glasses, respectively.

In the model of Oelkers et al. (1994), the forward dissolution rate r_+ is given by the following (eqn. 14 of Oelkers et al., 1994):

$$r_+ = k \frac{\left(\frac{a_{H^+}^{3s}}{a_{Al^{3+}}^s} \right) \prod_i a_{A_i}^{z_i}}{1 + K \left(\frac{a_{H^+}^{3s}}{a_{Al^{3+}}^s} \right) \prod_i a_{A_i}^{z_i}}, \quad (7)$$

where k is the effective dissolution rate constant, and K is the equilibrium constant for the exchange of Al and H on the mineral surface according to Oelkers et al. (1994, eqn. 10):



Here $a_i^{z_i}$ refers to the activities of the subscripted species i and x_i represents the stoichiometric coefficient of the species in Eqn. 8. In the latter equation, $M - sAl$ designates an Al-filled mineral surface site using the authors' original notation, but that we would infer to be a $Q_3^Si Q_3^{Al}$ site, s refers to a stoichiometric coefficient equal to the number of aluminum ions exchanged to create a surface precursor site, A_i stands for the i th aqueous species involved in the formation of the precursor, z_i represents stoichiometric coefficients for these aqueous species, and P represents the precursor species. The forward rate of dissolution is proportional to the concentration of P (Wieland et al., 1988). Oelkers et al. (1994) argue that this precursor site is an Al-deficient $SiOSi$ -linked site at all pH values. Again inferring from their argument and using our notation, P would be a $Q_v^Si Q_w^Si$ ($v = 2, w \leq 4$) site. The hydrolysis of the bridging oxygen in the $Q_3^Al Q_3^{Si}$ via reaction 8 should leave three precursor species regardless of glass composition; therefore, the values of v ($=2$) and s ($=1/3$) would be independent of glass composition (Oelkers, personal communication).

For conditions under which the activity of the precursor site before loss of Al, $\{M - sAl\}$, is much greater than $\{P\}$, Oelkers et al. (1994) simplified Eqn. 7 to

$$r_+ = k \left(\frac{a_{H^+}^{3s}}{a_{Al^{3+}}^s} \right) \prod_i a_{A_i}^{z_i} \quad (9)$$

(Oelkers et al., 1994, eqn. 16a) and rewrote this expression in terms of the measured total aqueous concentration of Al, $[Al_{tot}]$, and the dissociation constants and activity coefficients for aluminum hydroxide complexes in solution (Oelkers et al., 1994, eqn. 17):

$$r_+ = k \frac{\prod_i a_{A_i}^{z_i}}{[Al_{tot}]^s} \left(\frac{1}{\gamma_{Al^{3+}}} a_{H^+}^3 + \frac{K_{Al(OH)^+2}}{\gamma_{Al(OH)^+2}} a_{H^+}^2 + \frac{K_{Al(OH)_2^+}}{\gamma_{Al(OH)_2^+}} a_{H^+} + \frac{K_{Al(OH)_3^0}}{\gamma_{Al(OH)_3^0}} + \frac{K_{Al(OH)_4^-}}{\gamma_{Al(OH)_4^-}} a_{H^+}^{-1} \right)^s. \quad (10)$$

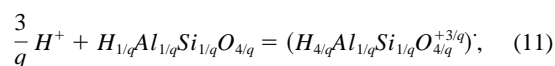
This model therefore predicts that dissolution rates should have an inverse dependence on Al concentration in solution. The

dissolution rate law is also based on the assumption that the same precursor site controls dissolution over the full range of pH.

To evaluate our data within the context of this model, we used values for the dissociation constants for aluminum hydroxide complexes reported by Castet et al. (1993) and assumed that $z_i = 0$ for all species other than H_2O . This latter assumption follows Oelkers et al. (1994), although Stillings and Brantley (1995), for example, found that rates of dissolution of feldspars decrease with increasing dissolved Na^+ . Given the generally linear release rates of Si vs. time observed here in batch experiments, we assumed that the effect of this cation (here present at the highest concentrations of 5, 2, and 0.06 mM in nepheline, jadeite, and albite pH 1 experiments, respectively) is minimal as compared to 0.01 mol/L NaCl in Stillings and Brantley (1995). We assumed that the activity coefficients for these complexes are all equal to one (all assumptions following Oelkers et al., 1994). We also assumed that the coefficient s did not vary with Al/Si ratio of the glass: $s = 0.33$ for albite, jadeite, and nepheline (Oelkers, personal communication). The only fit parameter remaining in the equation is k . The concentration of Al measured in solution at the end of each batch experiment was used as $[Al_{tot}]$ in the calculations.

By use of the Oelkers et al. (1994) approach, our model results are compared to the experimental results in Figure 8 on diagrams of $\log(\text{rate} \times [Al_{tot}]^s)$ vs. pH. For completeness, we present data and calculations for nepheline glass even though Oelkers and Schott (1995) and Schott and Oelkers (1995) derive another model for phases with Al/Si = 1 (see discussion below). The experimental results are plotted by means of the experimentally derived normalized dissolution rates reported in Table 2 and the same values for $[Al_{tot}]$ and s that are used in the model. The slopes of the experimental and calculated curves are compared in the caption of Figure 8. For the albite and jadeite, the calculated curves exhibit a steeper and somewhat shallower slope than the data at low and high pH, respectively. Although predicted slopes generally differ substantially from the experimental slopes, the model predicts that the slope of the dissolution curve from pH 1 to 4 becomes more shallow from jadeite to albite glass in a manner consistent with the experimental observations. In addition, the model predicts that slopes at high pH for both glasses are similar.

According to Oelkers and Schott (1995) and Schott and Oelkers (1995), a mineral such as anorthite (or nepheline) with Al/Si = 1 will dissolve by a different reaction because the removal of an Al atom leaves completely detached Si tetrahedra. For dissolution under acidic conditions, Oelkers and Schott (1995, eqn. 9) suggest reaction to form a single precursor complex:



in which q designates the number of precursor complexes formed by the adsorption of three hydrogens, $H_{1/q} Al_{1/q} Si_{1/q} O_{4/q}$ represents a hydrogenated surface site, and $H_{4/q} Al_{1/q} Si_{1/q} O_{4/q}^{+3/q}$ stands for a single precursor complex. The exchange of hydrogens for Al and development of the precursor then leads to the release of both Si and Al into solution. The associated rate law (Oelkers and Schott, 1995, eqn. 13) is

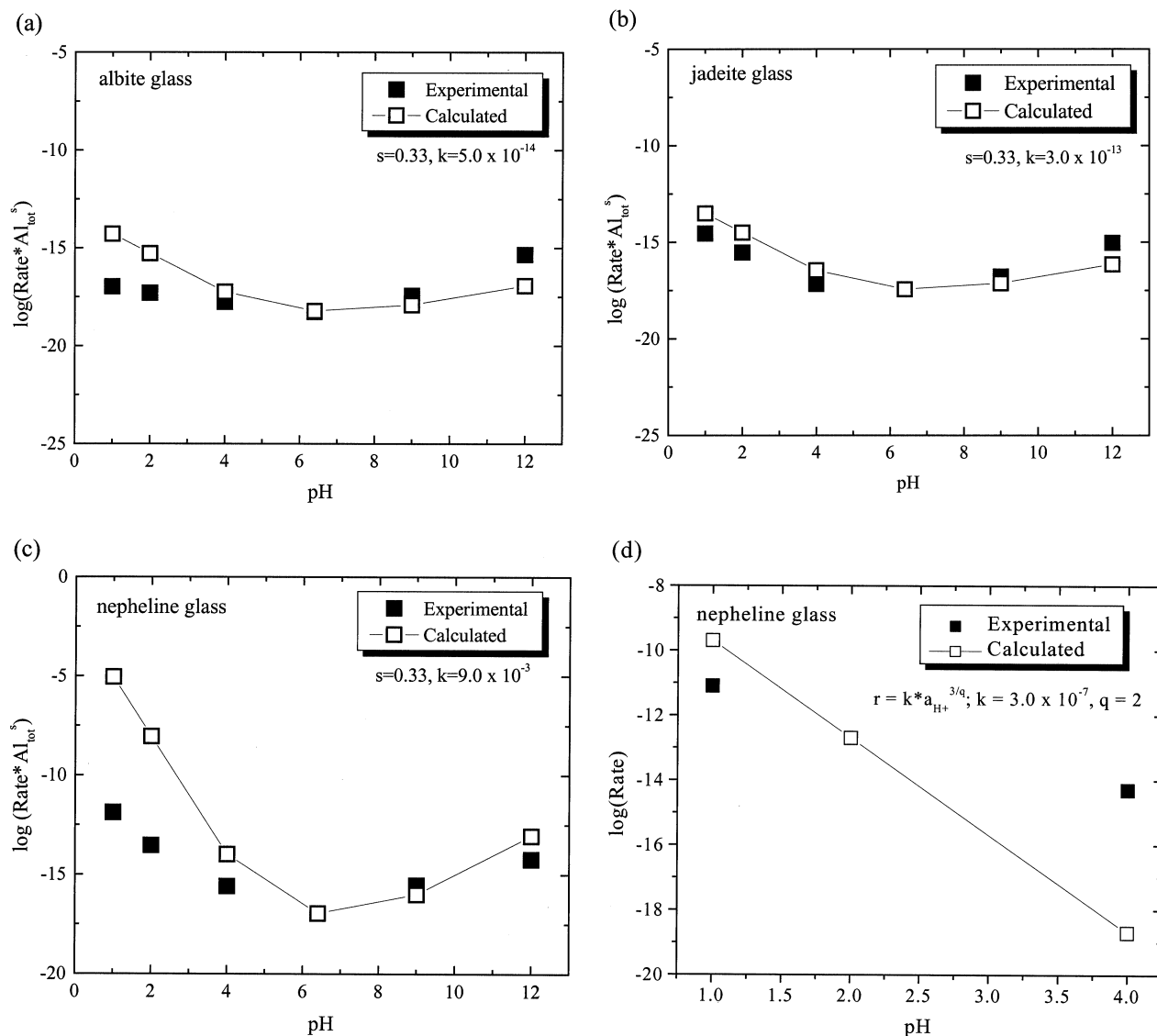


Fig. 8. Experimental data for dissolution of (a) albite glass, (b) jadeite glass, and (c) nepheline glass plotted together with calculated rates based on the model of Oelkers et al. (1994) as described in the text. Experimental data for nepheline dissolution is also plotted (d) together with calculated rates based on the model of Oelkers and Schott (1995) and Schott and Oelkers (1995). Slopes for (a) are -0.26 and 0.52 (experimental) and -0.98 and 0.23 (calculated) for acid and base, respectively. Slopes for (b) are -0.86 and 0.43 (experimental) and -0.98 and 0.23 (calculated) for acid and base, respectively. Slopes for (c) are -1.21 and 0.49 (experimental) and -2.98 and 0.71 (calculated) for acid and base, respectively. Slopes for (d) are -1.03 (experimental) and -3.00 (calculated).

$$r_+ = k_+ \frac{a_{\text{H}^+}^{3/q}}{1 + K_+ a_{\text{H}^+}^{3/q}} \quad (12)$$

If $K_+ a_{\text{H}^+}^{3/q} \ll 1$, then

$$r_+ = k_+ a_{\text{H}^+}^{3/q} \quad (13)$$

(Oelkers and Schott, 1995, eqn. 15). Eqn. 13 suggests that the dissolution rates far from equilibrium for minerals with $\text{Al}/\text{Si} = 1$ are strictly a function of aqueous hydrogen activity. The data for nepheline glass dissolution was therefore examined by this model proposed by Oelkers and Schott (1995) for anorthite dissolution.

Different values for q in Eqs. (11 to 13) have been used to describe anorthite dissolution data: Oelkers and Schott (1995) used $q = 2$, Amrhein and Suarez (1988) used $q = 1$, and Sverdrup (1990) used $q = 3$. The value of q is determined from measurement of the pH dependence of anorthite dissolution rates. Unfortunately, the experimental data of Oelkers and Schott (1995), Amrhein and Suarez (1988), and Sverdrup (1990) exhibit different pH dependencies and the reason for this discrepancy is unclear. Two possibilities are that the experimental data sets were collected at different temperatures and over narrow pH ranges. A comparison of the nepheline dissolution data for acidic pH values (1, 2, 4) and calculations

that used $q = 2$ following Oelkers and Schott (1995) is illustrated in Figure 8d. The model predicts the dependence on pH for dissolution of nepheline at low pH. However, this predicted slope is lower than the slope predicted by the other model for nepheline dissolution at low pH, contrary to experimental observations.

In effect, the two models (i.e., alkali feldspar (Oelkers et al., 1994) vs. anorthite (Oelkers and Schott, 1995)) differ in that the first assumes that the precursor site contains no Al, whereas the second assumes an Al-containing precursor. Oelkers and Schott (2001) suggest that their first model describes dissolution wherever Al-H⁺ exchange occurs—causing a dependence of the dissolution rate on Al in solution—whereas the second model explains phases where H⁺ adsorption only is necessary as a precursor to dissolution. For these latter phases, Al in solution is not observed to affect dissolution. Although we saw little evidence after the first several hundred hours for curvature in dissolution rate vs. time for most phases, Oelkers et al. (2001) have suggested that batch experiments must be analyzed by plotting log [Si] vs log t to determine strict linearity; they furthermore point out that slopes of such plots (b in Eqn. 4) should equal 0.75 for an Al dependence such as described in Eqn. 10. Data collected here yield values of b equal to 1 within 90% confidence for nepheline experiments except those at pH 9 and 12; for jadeite experiments except at pH 1, 4, 6, 9, and 12; and for albite experiments except at pH 6, 9, and 12. For the exceptions, b values as low as 0.75 cannot be discounted. Clearly, batch experiments such as ours are not easily interpreted in terms of the effect of [Al] on dissolution.

Several other observations from our study may contradict assumptions or implications of the models of Oelkers and coworkers. First, Oelkers and Schott (1995) predict identical pH slopes for all feldspars of composition up to 70% An, and by implication, for albite and jadeite glasses. In contrast, at low pH, the pH dependence measured here varied from glass to glass. Second, at high pH where our three glasses showed a similar pH dependence, the model of Oelkers and Schott (1995) is inferred to predict a different pH dependence for nepheline glass than for albite and jadeite because a different mechanism is inferred by those authors for a phase such as nepheline. Third, the increase in log (dissolution rate) vs. Al/Si content of the glasses studied here increases smoothly from albite to nepheline (Fig. 3) or remains constant at every pH, perhaps indicating the same mechanism controls dissolution for the glasses, albeit different mechanisms at high and low pH. To resolve these questions, further investigation through ab initio calculations should investigate the relative rates of hydrolysis of the Q_4 , Q_3 , Q_2 , and Q_1 species and further measurements of glass dissolution rates as a function of composition should be completed.

5. CONCLUSIONS

Three glasses with variable Al/Si, NaAlSi₃O₈, NaAlSi₂O₆, and NaAlSiO₄ were synthesized and dissolved over a range of pH. These three glasses are also of interest because they have mineral analogs: albite, jadeite, and nepheline, respectively, and because they allow investigation of the effects of variable Al/Si ratio without variation in Na/Ca or the presence of crystallographic defects. Many similarities in dissolution behavior between crystals of plagioclase composition and glasses

of the composition were observed: 1) dissolution was slowest at near-neutral pH and increased under acid and basic conditions; 2) dissolution rate at all pH values increased with increasing Al/Si ratio; 3) the pH dependence of dissolution was higher for the phase with Al/Si = 1 than the phase with Al/Si = 0.3; 4) after acid leaching, the extent of Al depletion of the altered surface increased with increasing bulk Al/Si ratio from Al/Si = 0.3 (albite) to 0.5 (jadeite), but then decreased in nepheline (Al/Si = 1.0), which dissolved stoichiometrically with respect to Al; and 5) little to no Al depletion of the surface occurred at pH > 7. These results may imply that conclusions drawn from our investigation may be extrapolated toward understanding the mechanism of dissolution of crystals of plagioclase composition.

One interpretation of the measured dissolution rates is that they are consistent with an identical mechanism controlling dissolution of nepheline, albite, and jadeite (and, by inference, plagioclase compositions), albeit by different mechanisms at high and low pH. Such a conclusion would be consistent with a transition state for all these aluminosilicates consisting of a protonated bridging oxygen between Q_4^{Al} and Q_4^{Si} at low pH and a deprotonated silanol group or a five-coordinate Si site after nucleophilic attack by OH^- at high pH. This possible mechanism for low pH dissolution would suggest that $Q_4^{Si}Q_4^{Si}$ linkages are slower to hydrolyze than $Q_4^{Al}Q_4^{Si}$, whereas all other linkages (e.g., $Q_v^{Si}Q_w^{Si}$, $Q_v^{Si}Q_w^{Al}$, $v, w \leq 3$) are easier to hydrolyze than either Q_4Q_4 linkages. Geometry optimizations that used ab initio methods for species inferred to be present in these glasses show that hydrolysis of AlOSi bonds becomes more energetically favorable as the number of Al atoms per Si tetrahedral increases, explaining why dissolution rates increase from albite to jadeite in nepheline glass. However, the development of Si-rich leached layers on acid-leached glasses may be more consistent with a rate limiting step of hydrolysis of $Q_v^{Si}Q_w^{Si}$ ($v, w \leq 3$) linkages. In that context, a model such as that of Oelkers et al. (1994) wherein $Q_4^{Al}Q_4^{Si}$ linkages are faster to hydrolyze than lower connectivity linkages between Si atoms was tested and found to explain some aspects of this data. In the context of that model, the mechanism of dissolution of nepheline would be interpreted to differ from that of albite and jadeite (Oelkers and Schott, 1995). Further computational and experimental measurements are needed to discriminate between the outstanding models. However, the use of glasses of variable composition to investigate these questions should shed light on the mechanisms of dissolution of aluminosilicate minerals.

Acknowledgments—The authors would like to thank H. Gong, S. Wu, M. Angelone, and V. Bojan of the Materials Characterization Laboratory and D. Voigt of the Department of Geosciences at Penn State University for assistance with sample characterization and experimental design. Reviews by R. Hellmann, R. Wogelius, E. Oelkers and one anonymous reviewer greatly benefitted the manuscript. This research was supported by the Department of Energy (DE-FG02-95ER14547.A000).

Associate editor: D. J. Wesolowski

REFERENCES

- Amrhein C. and Suarez D. L. (1988) The use of a surface complexation model to describe the kinetics of ligand-promoted dissolution of anorthite. *Geochim. Cosmochim. Acta* **52**, 2785–2793.
- Amrhein C. and Suarez D. L. (1992) Some factors affecting the

- dissolution kinetics of anorthite at 25°C. *Geochim. Cosmochim. Acta* **56**, 1815–1826.
- Bacon F. (1968) The chemical durability of silicate glass. *Glass Ind.* **49**, 438–559.
- Blum A. E. and Lasaga A. C. (1988) Role of surface speciation in the low-temperature dissolution of minerals. *Nature* **331**, 431–433.
- Blum A. E. and Lasaga A. C. (1991) The role of surface species in the dissolution of albite. *Geochim. Cosmochim. Acta* **55**, 2193–2201.
- Blum A. E. and Stillings L. L. (1995) Feldspar dissolution kinetics. In *Chemical Weathering Rates of Silicate Minerals* (eds. A. F. White and S. L. Brantley), *Reviews in Mineralogy*, Vol. 31, pp. 291–351. Mineral. Soc. Am.
- Brady P. V. and Walther J. V. (1992) Surface chemistry and silicate dissolution at elevated temperatures. *Am. J. Sci.* **29**, 639–658.
- Bland H. V., Curtiss L. A., and Iton L. E. (1993) Ab initio molecular orbital cluster studies of the zeolite ZSM-5: 1. Proton affinities. *J. Phys. Chem.* **97**, 12773–12782.
- Brantley S. L. and Stillings L. (1996) Feldspar dissolution at 25°C and low pH. *Am. J. Sci.* **296**, 101–127.
- Brantley S. L. and Stillings L. (1997) Reply: Feldspar dissolution at 25°C and low pH. *Am. J. Sci.* **297**, 1021–1032.
- Brückner R., Chun H.-U., and Goretzki H. (1978) Photoelectron spectroscopy (ESCA) on alkali silicate- and soda aluminosilicate glasses. *Glastech. Ber.* **51**, 1–7.
- Bunker B. C., Tallant D. R., and Headley T. J. (1988) The structure of leached sodium borosilicate glass. *Phys. Chem. Glasses* **29**, 106–120.
- Casey W. H., Westrich H. R., and Holdren G. R. (1991) Dissolution rates of plagioclase at pH = 2 and 3. *Am. Mineral.* **76**, 211–217.
- Castet S., Danduran J. L., Schott J., and Gout R. (1993) Boehmite solubility and aqueous aluminum speciation in hydrothermal solutions (90–350°C): Experimental study and modeling. *Geochim. Cosmochim. Acta* **57**, 4869–4884.
- Chou L. and Wollast R. (1985) Steady-state kinetics and dissolution mechanisms of albite. *Am. J. Sci.* **285**, 963–993.
- Clark D. E., Pantano C. G., and Hench L. L. (1979) *Corrosion of Glass*. Books for Industry.
- Clark D. E. and Zaitos B. K., eds. (1992) *Corrosion of Glass, Ceramics and Ceramic Superconductors*. Noyes Publications.
- Day D. E. and Rindone G. E. (1962) Properties of soda aluminosilicate glasses: I, refractive index, density, molar refractivity, and infrared absorption spectra. *J. Am. Ceram. Soc.* **45**, 489–496.
- Dirken P. J., Kohn S. C., Smith M. E., and van Eck E. R. H. (1997) Complete resolution of Si-O-Si and Si-O-Al fragments in an aluminosilicate glass by ¹⁷O multiple quantum magic angle spinning NMR spectroscopy. *Chem. Physics Lett.* **266**, 568–574.
- Doremus R. H. (1975) Interdiffusion of hydrogen and alkali ions in a glass surface. *J. Non-Cryst. Solids* **19**, 137–144.
- Doremus R. H. (1980) Infrared spectroscopy of surfaces of glasses containing alkali ions. *J. Non-Cryst. Solids* **41**, 145–149.
- Doremus R. H. (1994) Chemical durability: Reaction of water with glass. In *Glass Science*, 2nd ed., pp. 215–240. Wiley.
- Douglas R. W. and El-Shamy T. M. M. (1967) Reactions of glasses with aqueous solutions. *J. Am. Ceram. Soc.* **50**, 1–8.
- Dubrovo S. K. (1954a) Reaction of vitreous sodium silicates and aluminosilicates with aqueous solutions. Communication 3. Effect of the addition of silica and alumina to sodium silicates on the instability of the latter to acids. *Bull. Acad. Sci. USSR Div. Chem. Sci.* T197–T203.
- Dubrovo S. K. (1954b) Reaction of vitreous sodium silicates and aluminosilicates with aqueous solutions. Communication 4. Reaction of vitreous sodium aluminosilicates with solutions of acids. *Bull. Acad. Sci. USSR Div. Chem. Sci.* T661–T668.
- Dubrovo S. K. (1958) Reaction of glassy sodium silicates and aluminosilicates with aqueous solutions. Communication 8. Action of acid solutions on glassy sodium aluminosilicates with variable acid number. *Bull. Acad. Sci. USSR Div. Chem. Sci.* T1117–T1123.
- Dubrovo S. K. and Shmidt Y. A. (1953) Reaction of vitreous silicates and aluminosilicates with aqueous solutions. Communication 1. Reactions of vitreous sodium silicates with water and with hydrochloric acid solutions. *Bull. Acad. Sci. USSR Div. Chem. Sci.* T535–T543.
- Dubrovo S. K. and Shmidt Y. A. (1955a) Reaction of vitreous silicates and aluminosilicates with aqueous solutions. Communication 6. Reaction of vitreous sodium silicates and aluminosilicates with caustic alkali solutions. *Bull. Acad. Sci. USSR Div. Chem. Sci.* T359–T364.
- Dubrovo S. K. and Shmidt Y. A. (1955b) Reaction of vitreous silicates and aluminosilicates with aqueous solutions. Communication 7. Reaction of vitreous sodium silicates and aluminosilicates with salt solutions. *Bull. Acad. Sci. USSR Div. Chem. Sci.* T539–T544.
- Eggleston C. M., Hochella M. F. Jr., and Parks G. A. (1989) Sample preparation and aging effects on the dissolution rate and surface composition of diopside. *Geochim. Cosmochim. Acta* **53**, 797–805.
- El-Shamy T. M., Lewins J., and Douglas R. W. (1972) The dependence on the pH of the decomposition of glasses by aqueous solutions. *Glass Technol.* **13**, 81–87.
- Fleer V. N. (1982) The dissolution kinetics of anorthite (CaAl₂Si₂O₈) and synthetic strontium feldspar (SrAl₂Si₂O₈) in aqueous solutions at temperatures below 100°C: Applications to the geological disposal of radioactive nuclear wastes. Ph.D. thesis, Pennsylvania State University, University Park.
- Frisch M. J., Trucks G. W., Schlegel H. B., Scuseria G. E., Robb M. A., Cheeseman J. R., Zakrzewski V. G., Montgomery J. A., Stratmann R. E., Burant J. C., Dapprich S., Millam J. M., Daniels A. D., Kudin K. N., Strain M. C., Farkas O., Tomasi J., Barone V., Cossi M., Cammi R., Mennucci B., Pomelli C., Adamo C., Clifford S., Ochterski J., Petersson G. A., Ayala P. Y., Cui Q., Morokuma K., Malick D. K., Rabuck A. D., Raghavachari K., Foresman J. B., Cioslowski J., Ortiz J. V., Stefanov B. B., Liu G., Liashenko A., Piskorz P., Komaromi I., Gomperts R., Martin R. L., Fox D. J., Keith T., Al-Laham M. A., Peng C. Y., Nanayakkara A., Gonzalez C., Challacombe M., Gill P. M. W., Johnson B. G., Chen W., Wong M. W., Andres J. L., Head Gordon M., Replogle E. S., and Pople J. A. (1998) Gaussian 98. Gaussian Inc.
- Geisinger K. L., Gibbs G. V., and Navrotsky A. (1985) A molecular orbital study of bond length and angle variations in framework structures. *Phys. Chem. Minerals* **11**, 266–283.
- Geotti-Bianchini F., Riu L. D., Gagliardi G., Guglielmi M., and Pantano C. G. (1991) New interpretation of the IR reflectance spectra of SiO₂-rich films on soda-lime glass. *Glastech. Ber.* **64**, 205–217.
- Goldman D. S. (1986) Evaluation of the ratios of bridging to non-bridging oxygens in simple silicate glasses by electron spectroscopy for chemical analysis (ESCA). *Phys. Chem. Glasses* **27**, 128–133.
- Grambow B. (1992) Geochemical approach to glass dissolution. In *Corrosion of Glass, Ceramics and Ceramic Superconductors* (eds. D. E. Clark and B. K. Zaitos), pp. 124–152. Noyes Publications.
- Guiton T. A. (1991) Infrared reflectance spectroscopy of porous silicas. Ph.D. thesis, Pennsylvania State University, University Park.
- Guiton T. A. (1993) Infrared reflectance spectroscopy of porous silicas. *Coll. Surf. A* **74**, 33–46.
- Hamilton J. P., Pantano C. G., and Brantley S. L. (2000) Dissolution rates of albite crystal and glass. *Geochim. Cosmochim. Acta* **64**, 2603–2615.
- Helgeson H. C. (1971) Kinetics of mass transfer among silicates and aqueous solutions. *Geochim. Cosmochim. Acta* **35**, 421–469.
- Helgeson H. C., Murphy W. M., and Aagaard P. (1984) Thermodynamic and kinetic constraints on reaction rates among minerals and aqueous solutions. II. Rate constants, effective surface area, and the hydrolysis of feldspar. *Geochim. Cosmochim. Acta* **48**, 2405–2432.
- Murphy W. M. and Helgeson H. C. (1987) Thermodynamic and kinetic constraints on reaction rates among minerals and aqueous solutions. III. Activated complexes and the pH-dependence of the rates of feldspar, pyroxene, wollastonite, and olivine hydrolysis. *Geochim. Cosmochim. Acta* **51**, 3137–3153.
- Hellmann R. (1994) The albite–water system: Part I. The kinetics of dissolution as a function of pH at 100, 200, and 300°C. *Geochim. Cosmochim. Acta* **58**, 595–611.
- Hellmann R. (1995) The albite–water system: Part II. The time-evolution of the stoichiometry of dissolution as a function of pH at 100, 200, and 300°C. *Geochim. Cosmochim. Acta* **59**, 1669–1697.
- Hellmann R. (1997) The albite–water system: Part IV. Diffusion modeling of leached and hydrogen-enriched layers. *Geochim. Cosmochim. Acta* **61**, 1595–1611.
- Hellmann R., Eggleston C. M., Hochella M. F., and Crerar D. A. (1990) The formation of leached layers on albite surfaces during dissolution under hydrothermal conditions. *Geochim. Cosmochim. Acta* **54**, 1267–1281.
- Hench L. L. and Clark D. E. (1978) Physical chemistry of glass surfaces. *J. Non-Cryst. Solids* **28**, 83–105.

- Holdren G. R. and Speyer P. M. (1987) Reaction rate surface area relationships during the early stages of weathering. II. Data on eight additional feldspars. *Geochim. Cosmochim. Acta* **51**, 2311–2318.
- Hsieh C. H., Jain H., Miller A. C., and Kamitsos E. I. (1994) X-ray photoelectron spectroscopy of Al- and B-substituted sodium trisilicate glasses. *J. Non-Cryst. Solids* **168**, 247–257.
- Husung R. D. and Doremus R. H. (1990) The infrared transmission spectra of four silicate glasses before and after exposure to water. *J. Mater. Res.* **5**, 2209–2217.
- Kerly T. A. (1983) Corrosion of sodium-aluminosilicate glasses. M.Sc. thesis. Pennsylvania State University, University Park.
- Kubicki J. D. and Sykes D. (1993) Molecular orbital calculations of vibrations in three-membered aluminosilicate rings. *Phys. Chem. Mineral.* **19**, 381–391.
- Kubicki J. D., Xiao Y., and Lasaga A. C. (1993) Theoretical reaction pathways for the formation of $[\text{Si}(\text{OH})_3]^{1-}$ and the deprotonation of orthosilicic acid in basic solution. *Geochim. Cosmochim. Acta* **57**, 3847–3853.
- Kubicki J. D., Blake G. A., and Apitz S. E. (1996) Ab initio calculations on aluminosilicate Q3 species: Implications for atomic structures of mineral surfaces and dissolution mechanisms of feldspars. *Am. Mineral.* **81**, 789–799.
- Lee S. K. and Stebbins J. (1999) The degree of aluminum avoidance in aluminosilicate glasses. *Am. Mineral.* **84**, 937–945.
- Loewenstein W. (1954) The distribution of aluminum in the tetrahedral of silicates and aluminates. *Am. Mineral.* **39**, 92–96.
- Mast M. A. and Drever J. I. (1987) The effect of oxalate on the dissolution rates of oligoclase and tremolite. *Geochim. Cosmochim. Acta* **51**, 2559–2568.
- Melnyk T. W., Walton F. B., and Johnson H. L. (1983) *High-Level Waste Glass Field Burial Tests at CRNL: The Effect of Geochemical Kinetics on the Release and Migration of Fission Products in a Sandy Aquifer*. Atomic Energy of Canada Limited (AECL-6836), Whiteshell Nuclear Research Establishment.
- Muir I. J., Bancroft G. M., Shotyk W., and Nesbitt H. W. (1990) A SIMS and XPS study of dissolving plagioclase. *Geochim. Cosmochim. Acta* **54**, 2247–2256.
- Oelkers E. H., Schott J., and Devidal J.-L. (1994) The effect of aluminum, pH, and chemical affinity on the rates of aluminosilicate dissolution reactions. *Geochim. Cosmochim. Acta* **58**, 2011–2024.
- Oelkers E. H. and Schott J. (1995) Experimental study of anorthite dissolution and the relative mechanism of feldspar hydrolysis. *Geochim. Cosmochim. Acta* **59**, 5039–5053.
- Oelkers E. H. and Schott J. (2001) An experimental study of enstatite dissolution rates as a function of pH, temperature, and aqueous Mg and Si concentration, and the mechanism of pyroxene/pyroxenoid dissolution. *Geochim. Cosmochim. Acta* **59**, 1219–1231.
- Oelkers E. H., Schott J., and Devidal D.-L. (In press) Comment: On the interpretation of closed system mineral dissolution experiments [comment on "Mechanism of kaolinite dissolution at room temperature and pressure, part II: Kinetic study," by F. J. Huertas, L. Chou, and R. Wollast]. *Geochim. Cosmochim. Acta*.
- Onorato P. I. K., Alexander M. N., Struck C. W., Tasker G. W., and Uhlmann D. R. (1985) Bridging and nonbridging oxygen atoms in alkali aluminosilicate glasses. *J. Am. Ceram. Soc.* **68**, C148–C150.
- Oxburgh R., Drever J. I., and Sun Y. T. (1994) Mechanism of plagioclase dissolution in acid solution at 25°C. *Geochim. Cosmochim. Acta* **58**, 661–670.
- Pelmenschikov A., Strandh H., Pettersson L. G. M., and Leszczynski J. (2000) Lattice resistance to hydrolysis of SiO_4 bonds of silicate minerals: Ab initio calculations of a single water attack onto the (001) and (111)-cristobalite surfaces. *J. Phys. Chem. B* **104**, 5779–5783.
- Roy B. N. (1990) Infrared spectroscopy of lead and alkaline-earth aluminosilicate glasses. *J. Am. Ceram. Soc.* **73**, 846–855.
- Sanders D. M., Person W. B., and Hench L. L. (1974) Quantitative analysis of glass structure with the use of infrared reflectance spectra. *Appl. Spectrosc.* **28**, 247–255.
- Seah M. P. and Dench W. A. (1979) Quantitative electron spectroscopy of surfaces: A standard data base for electron inelastic mean free paths in solids. *Surface Interface Anal.* **1**, 2–11.
- Schott J. (1990) Modeling of the dissolution of strained and unstrained multiple oxides: The surface speciation approach. In *Aquatic Chemical Kinetics* (ed. W. Stumm), pp. 337–365. Wiley.
- Schott J. and Oelkers E. H. (1995) Dissolution and crystallization rates of silicate minerals as a function of chemical affinity. *Pure Appl. Chem.* **67**, 903–910.
- Shelby J. E. (1978) Viscosity and thermal expansion of lithium-aluminosilicate glasses. *J. Appl. Phys.* **49**, 5885–5891.
- Shmidt Y. A. (1954a) Reaction of vitreous sodium silicates and aluminosilicates with aqueous solutions. Communication 2. Reaction of vitreous sodium disilicate with aqueous solutions. *Bull. Acad. Sci. USSR Div. Chem. Sci.* T191–T196.
- Shmidt Y. A. (1954b) Reaction of vitreous sodium silicates and aluminosilicates with aqueous solutions. Communication 5. Reaction of vitreous sodium aluminosilicates with water. *Bull. Acad. Sci. USSR Div. Chem. Sci.* T669–T673.
- Sjöberg L. (1989) Kinetics and non-stoichiometry of labradorite dissolution. In *Proc. 6th Intern. Symp.: On Water-Rock Interaction* (ed. D. L. Miles), pp. 609–612. Rotterdam: A. A. Balkema.
- Smets B. M. J. and Lommen T. P. A. (1981) The incorporation of aluminum oxide and boron oxide in sodium silicate glasses, studied by X-ray photoelectron spectroscopy. *Phys. Chem. Glasses* **22**, 158–162.
- Smets B. M. J. and Lommen T. P. A. (1982) The leaching of sodium aluminosilicate glasses studied by secondary ion mass spectrometry. *Phys. Chem. Glasses* **23**, 83–87.
- Stillings L. L. and Brantley S. L. (1995) Feldspar dissolution at 25°C and pH 3: Reaction stoichiometry and the effect of cations. *Geochim. Cosmochim. Acta* **59**, 1483–1496.
- Stumm W. and Morgan J. J. (1996) *Aquatic Chemistry; Chemical Equilibria and Rates in Natural Waters*. 3rd ed. Wiley.
- Sverdrup H. U. (1990) *The Kinetics of Base Cation Release Due to Chemical Weathering*. Lund University Press.
- Sykes D. and Kubicki J. D. (1993) A model for H_2O solubility mechanisms in albite melts from infrared spectroscopy and molecular orbital calculations. *Geochim. Cosmochim. Acta* **57**, 1039–1052.
- Sykes D. and Kubicki J. D. (1996) Four-membered rings in silica and aluminosilicate glasses. *Am. Mineral.* **81**, 265–272.
- Sykes D., Kubicki J. D., and Farrar T. C. (1997) Molecular orbital calculation of ^{27}Al and ^{29}Si NMR parameters in Q3 and Q4 aluminosilicate molecules and implications for the interpretation of hydrous aluminosilicate glass NMR spectra. *J. Phys. Chem.* **101**, 2715–2722.
- Taylor M. and Brown G. E. Jr. (1979a) Structure of mineral glasses—I. The feldspar glasses $\text{NaAlSi}_3\text{O}_8$, KAlSi_3O_8 , $\text{CaAl}_2\text{Si}_2\text{O}_8$. *Geochim. Cosmochim. Acta* **43**, 61–75.
- Taylor M. and Brown G. E. Jr. (1979b) Structure of mineral glasses—II. The SiO_2 - NaAlSiO_4 join. *Geochim. Cosmochim. Acta* **43**, 1467–1473.
- Tole M. P., Lasaga A. C., Pantano C. G., and White W. B. (1986) The kinetics of dissolution of nepheline (NaAlSiO_4). *Geochim. Cosmochim. Acta* **50**, 379–392.
- Vig J. R. (1992) *Ultraviolet-Ozone Cleaning of Semiconductor Surfaces*. Research and Development Technical Report SL CET-TR-91-33 (Rev. 1). Army Research Laboratory, Electronics and Power Sources Directorate.
- Walther J. V. (1996) Relation between rates of aluminosilicate mineral dissolution, pH, temperature, and surface charge. *Am. J. Sci.* **296**, 693–728.
- Walther J. V. (1997) Comment: Feldspar dissolution at 25°C and low pH. *Am. J. Sci.* **297**, 1012–1021.
- White W. B. (1992) Theory of corrosion of glass and ceramics. In *Corrosion of Glass, Ceramics and Ceramic Superconductors* (ed. D. E. Clark and B. K. Zaitos), pp. 2–28. Noyes Publications.
- White A. F. and Brantley S. L. (1995) *Chemical Weathering Rates of Silicate Minerals*. Mineralogical Society of America Short Course **31**, 1–22.
- Wieland E., Wehrli B., and Stumm W. (1988) The coordination chemistry of weathering: III. A generalization on the dissolution rates of minerals. *Geochim. Cosmochim. Acta* **52**, 1969–1981.
- Xiao Y. and Lasaga A. (1995) Ab initio quantum mechanical studies of the kinetics and mechanisms of silicate dissolution; H^+ (H_3O^+) catalysis. *Geochim. Cosmochim. Acta* **58**, 5379–5400.
- Zirl D. M. and Garofalini S. H. (1990) Structure of sodium aluminosilicate glasses. *J. Am. Ceram. Soc.* **73**, 2848–2856.